A NEW MODE OF CLASS D AMPLIFICATION

by

Philip M. Cowett, Jr.

Thesis submitted to the Graduate Faculty of the

Virginia Polytechnic Institute

in partial fulfillment of the requirements for the degree of

MASTER OF SCIENCE

in

Electrical Engineering

APPROVED:

C. A. Holt, Chairman

H. L. Krauss

H. H. Hull

W. A. Blackwell

May 1971

Blacksburg, Virginia

TABLE OF CONTENTS

LIST OF TABLES

LIST OF ILLUSTRATIONS

CHAPTER I

INTRODUCTION

With the current trend in electronics toward microminiaturization there is a need for a more efficient method of power amplification. The Class D principle, originally invented by B. D. Bedford in 1931 [1], is one method of satisfying this need.

In a Class D stage there is current for an average of 50% of the period, but unlike Class B, the amplifying device is fully saturated whenever current flows. Thus the transistor, tube, thyristor, etc. behaves as a switch, dissipating very little power. This saving of power is of little consequence with tube circuits, and for this reason the idea did not receive much attention until the invention of the transistor. It has been only recently that the Class D idea has been investigated again.

Amplification in a Class D system takes place by modulation of a series of constant-amplitude pulses. Amplitude modulation of the pulses is ruled out because the transistor switches are either "on" (saturated) or "off". The signal is recovered from the modulated pulses by means of a low-pass filter. Several types of modulation may be used with this scheme such as pulse-width (duration) modulation, pulse-frequency modulation, pulse-burst modulation, etc. Pulse-width modulation seems to be the simplest and, therefore, it is the most widely used method.

The output before filtering of a pulse-width-modulated amplifier with no input signal is a square wave at the switching frequency (generally several times higher than the highest modulation frequency)

with a 50% duty cycle as shown in Fig. 1.1(a). During positive portions of the modulating signal the top of the waveform is wider than the bottom, resulting in a net positive voltage, as indicated by the dashed line in Fig. 1.1(b). Figure 1.1(c) shows the output waveform for a net negative output signal. If these three pulse trains were passed through a low-pass filter, the output after the filter would be the dashed lines.

These pulses must be produced by some kind of push-pull output circuit to avoid dc power dissipation either in the load or in a resistor. A typical circuit used for this purpose is shown in Fig. 1.2.

This circuit has the advantage over others in that the drive is always removed from the top transistor before it is applied to the bottom one, and vice versa, reducing the possibility of both transistors being on at the same time. However, in higher power circuits it may be hard to find a suitable NPN-PNP pair, making it necessary to use a different configuration using both NPN's or both PNP's. This would require separate drives to each transistor, increasing the probability that both transistors will be on for a time. Even in the circuit of Fig. 1.2, chances are that the turn-off time of one transistor somewhat exceeds the turn-on time of the other. The instant when both transistors are on together results in high instantaneous collector current and high dissipation. This problem can be controlled by providing a slight time delay between turn-off of one transistor and turn-on of the other, but this delay would have to be adjusted for individual transistor differences, and the proper delay may vary over portions of the output cycle or with temperature. Use of a regenerative output

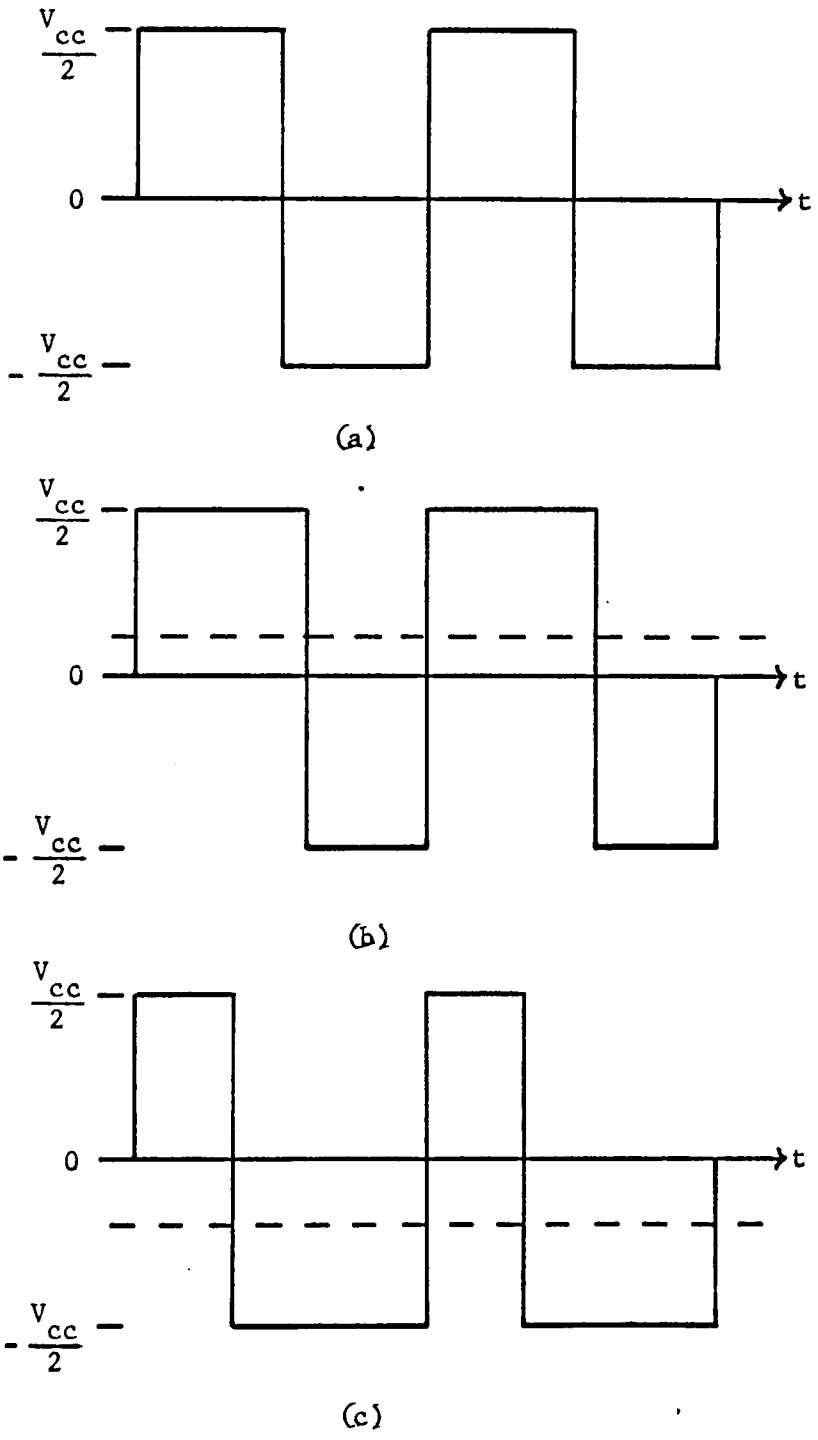

Fig. 1.1. Unfiltered output waveforms of pulse-width-modulated amplifier. Dashed lines represent average voltage level.

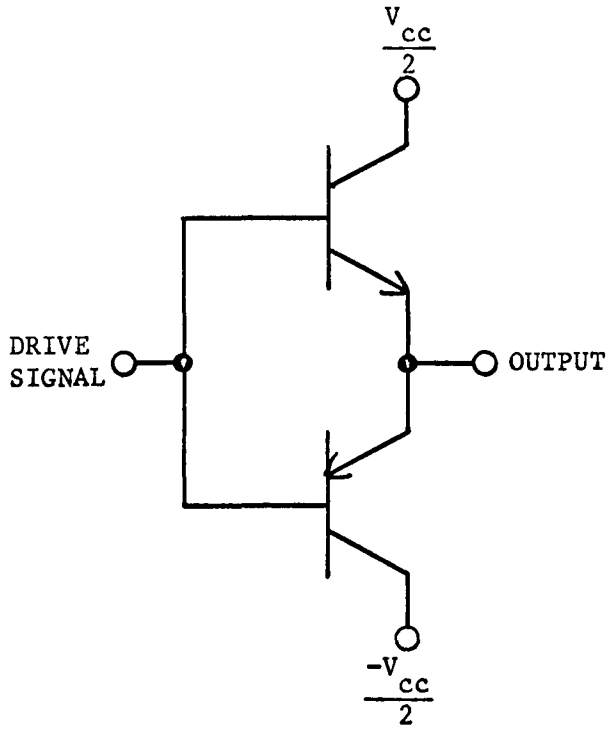

Fig. 1.2. Typical output stage used in Class D amplifier.

stage, as proposed by Birt [2], would help solve this problem but would present some design problems.

With no signal input the amplifier feeds a pure square wave at the switching frequency into the filter. As no practical filter is perfect, some of this voltage results in dissipation in both the filter and the load.

A mode of operation that reduces these problems was presented by Crowhurst [3]. In his system, under no-signal conditions, the unfiltered output is that shown in Fig. 1.3(b), compared with that of a conventional Class D amplifier (Fig. 1.3(a)).

Obviously, the voltage waveform of Fig. 1.3(b) has a much lower RMS value than that of Fig. 1.3(a). Also, there is ample time for one transistor to turn off before the other one turns on in the system having the output of Fig. 3(b). As the filtered output voltage becomes more positive, the positive pulses become wider while the negative ones become narrower and finally disappear. As the two pulses of Fig. 1.2 both have a maximum width of T and a minimum width of zero, the two systems are capable of the same dynamic range. The carrier (switching) frequency component of output has an RMS value that is so much lower in the mode of Fig. 1.3(b) that this waveform, when modulated, can be fed into a resistance load without filtering with an efficiency of about 50% (i.e., half of the load power is the desired modulation signal component).

Severe filtering problems are introduced using this new mode of operation, because of the large amount of time when both transistors are "off". These will be dealt with in detail. However, they can be

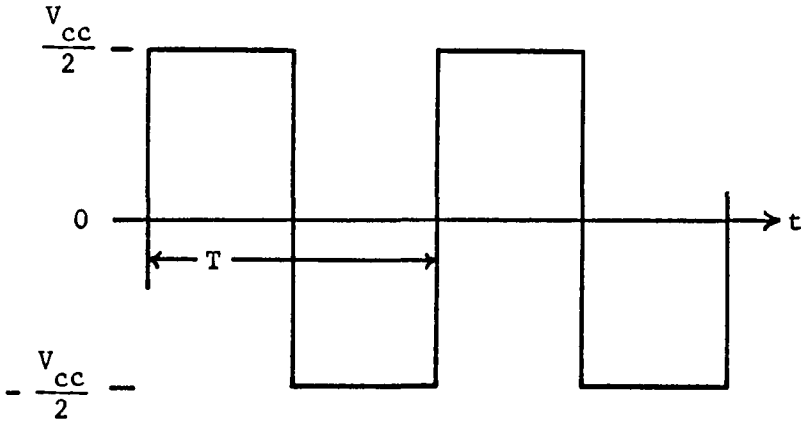

(a)

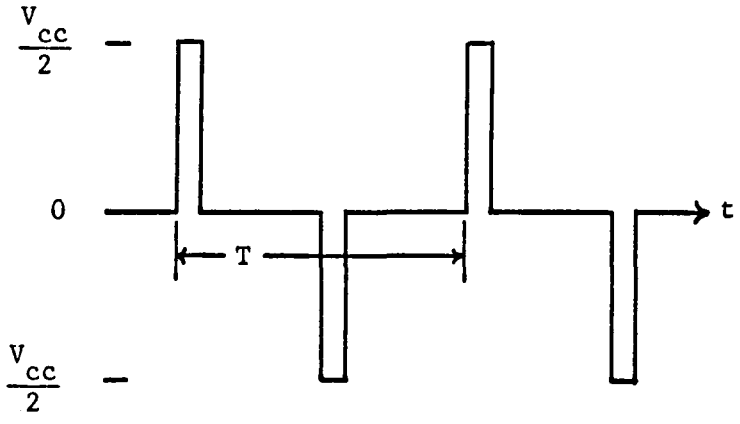

(b)

Fig. 1.3. Unfiltered no-signal output of Class D amplifier.
(a) Conventional. (b) New Mode.

partially overcome by use of a "damping" resistor in the filter (which results in only a slight reduction in efficiency) and negative feedback. The new mode is also less "upset" by the addition of a feedback signal containing a small switching-frequency component, thus permitting far greater amounts of feedback to be used.

This paper describes a 15-watt audio amplifier designed to operate in either mode. Efficiencies are considerably higher using the new mode, particularly when negative feedback is used.

CHAPTER II

THEORY OF CLASS D AMPLIFICATION

This chapter presents a review of the principles involved in conventional Class D amplification and a complete theoretical analysis of the New Mode of Class D amplification. The advantage of natural sampling over uniform sampling, and double-edge modulation over single-edge modulation, are discussed.

2.1 Conventional Class D Amplification

The pulse-width modulated wave, which is the unfiltered output of a Class D system, can be produced in a number of ways. All of them involve the combining of the input signal with a high-frequency ramp-type (triangle, sawtooth, etc.) sampling signal, and the passing of this signal through a slicer, which is a device whose output is one value for inputs less than a certain level and another value for inputs greater than that level. The sampling signal frequency must be at least twice the highest frequency to be amplified, and it is typically four or five times the highest frequency to be amplified.

The simplest and, therefore, most commonly used method of sampling is natural sampling. In natural sampling the input (modulating) signal is added directly to the sampling signal and the sum is passed through a slicer. This is shown graphically in Fig. 2.1.1, using a negative-going sawtooth wave as the sampling signal. This results in an output square wave with the leading edge fixed and the trailing edge modulated. The spectrum of this output according to Black [4], is

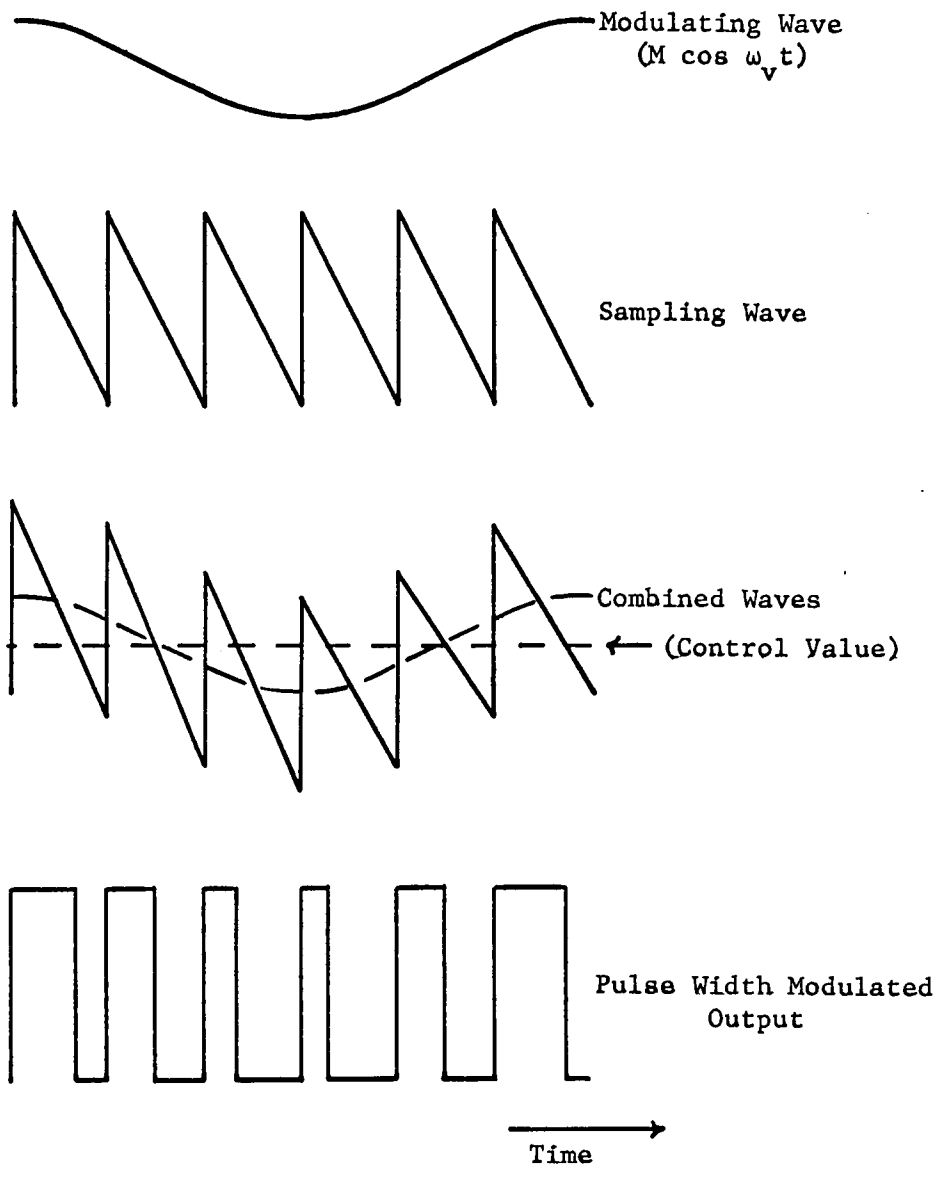

Fig. 2.1.1. Generation of PWM using natural sampling.

$$F_1(t) = k + \frac{M}{2}\cos(\omega_v t) + \sum_{m=1}^{\infty} \frac{\sin(m\omega_c t)}{m\pi}$$

$$- \sum_{m=1}^{\infty} \frac{J_o(m\pi M)}{m\pi} \sin(m\omega_c t - 2m\pi k)$$

$$- \sum_{m=1}^{\infty} \sum_{n=\pm 1}^{\pm\infty} \frac{J_n(m\pi M)}{m\pi} \sin(m\omega_c t + n\omega_v t - 2m\pi k - \frac{n\pi}{2}) \qquad (2.1.1)$$

where $M\cos(\omega_v t)$ is the modulating wave and ω_c is the sampling frequency. The modulation factor M is the ratio of peak modulation amplitude to peak carrier amplitude. The k term is the ratio of unmodulated pulse duration to the interval between pulse centers, this being 1/2 in this case. $J_n(m\pi M)$ is the nth-order Bessel function of $(m\pi M)$.

If a positive-going sawtooth is used as the sampling wave, pulse width modulation with leading edges modulated is produced. Its Fourier series is identical to that for trailing edges modulated but with the time scale reversed. Thus,

$$F_2(t) = F_1(-t) = k + \frac{M}{2}\cos(\omega_v t) - \sum_{m=1}^{\infty} \frac{\sin(m\omega_c t)}{m\pi}$$

$$+ \sum_{m=1}^{\infty} \frac{J_o(m\,M)}{m\pi} \sin(m\omega_c t + 2m\pi k)$$

$$+ \sum_{m=1}^{\infty} \sum_{n=\pm 1}^{\pm\infty} \frac{J_n(m\pi M)}{m\pi} \sin(m\omega_c t + n\omega_v t + 2m\pi k + \frac{n\pi}{2}) \qquad (2.1.2)$$

If an isoceles triangle wave is used as a modulating wave, the result is PWM with both edges modulated. This can be represented as the sum of two waves--one with trailing edges modulated and one with leading edges modulated. Thus,

$$F_3(t) = F_1(t)+F_2(t)$$

$$= 2k + M\cos(\omega_v t)+2\sum_{m=1}^{\infty}\frac{J_o(m\pi M)}{m\pi}\sin(2m\pi k)\cos(m\omega_c t)$$

$$+2\sum_{m=1}^{\infty}\sum_{n=\pm1}^{\infty}\frac{J_n(m\pi M)}{m\pi}\sin(2m\pi k+\frac{n\pi}{2})\cos(m\omega_c t+n\omega_v t) \qquad (2.1.3)$$

In this case M and k no longer retain their original definitions. If M exceeds a value of 0.5, the two modulated edges overlap. Thus substituting $\frac{M_d}{2}$ for M, and $\frac{k_d}{2}$ for k, would correct this. The subscript d refers to double-edge modulation.

To recover the original modulating signal, the PWM output of a Class D amplifier is passed through a low-pass filter, whose cutoff frequency is equal to the highest frequency to be amplified. With a filter input described by Eq. (2.1.1), the output of the filter would be

$$k+\frac{M}{2}\cos(\omega_v t)$$

$$+\{\text{those terms of}\left[\sum_{m=1}^{\infty}\sum_{n=\pm1}^{\pm\infty}\frac{J_n(m\pi M)}{m\pi}\sin(m\omega_c t+n\omega_v t-2m\pi k-\frac{n\pi}{2})\right]$$

such that $(m\omega_c+n\omega_v)$ < the filter cutoff frequency$\}$ (2.1.4)

The dc term k can be removed with a capacitor or with balanced circuit design. The term $\frac{M}{2}\cos(\omega_v t)$ is the desired modulation. The third expression contains terms of frequencies $(m\omega_c \pm n\omega_v)$. The amplitudes of these terms generally decrease with increasing m and n, so the only terms which contribute significant distortion inside the filter passband are those of frequencies $(\omega_c - n\omega_v)$.

The filtered output of Eq. (2.1.3), the double-edge modulation spectrum, is

$$k_d + \frac{M_d}{2} \cos(\omega_v t) + \{\text{those terms of} \left[\sum_{m=1}^{\infty} \sum_{n=\pm 1}^{\pm\infty} \frac{J_n(m\pi M_d)}{m\pi} \sin(m\pi k_d + \frac{n\pi}{2}) \cos(m\omega_c t + n\omega_v t) \right]$$

such that $(m\omega_c \pm n\omega_v)$ < the filter cutoff frequency$\}$ (2.1.5)

As before, the only significant distortion terms are those at frequencies of $(\omega_c - n\omega_v)$ which are inside the filter passband. However, for $k_d = 1/2$ (the usual case) the double summation goes to zero for even values of $(m+n)$, because it contains the factor $[\sin(1/2\, m\pi + 1/2\, n\pi)]$; thus for m=1, the terms are zero for m odd. In addition, the remaining terms for n even are reduced in amplitude compared with similar terms for single-edge modulation.

The other commonly used method of producing PWM is uniform sampling. Uniform sampling is accomplished by first converting the modulating signal to pulse-amplitude modulation as shown in Fig. 2.1.2. Note that all pulses are of equal width and there are no spaces between pulses. Next the sampling wave (as before, this can be a positive- or negative-going sawtooth or a triangle wave) is added to the PAM, and these combined waves are passed through a slicer.

According to Black [4], the spectrum of a pulse-width-modulated wave using uniform sampling and with trailing edges modulated (negative-going sawtooth used for sampling wave) is

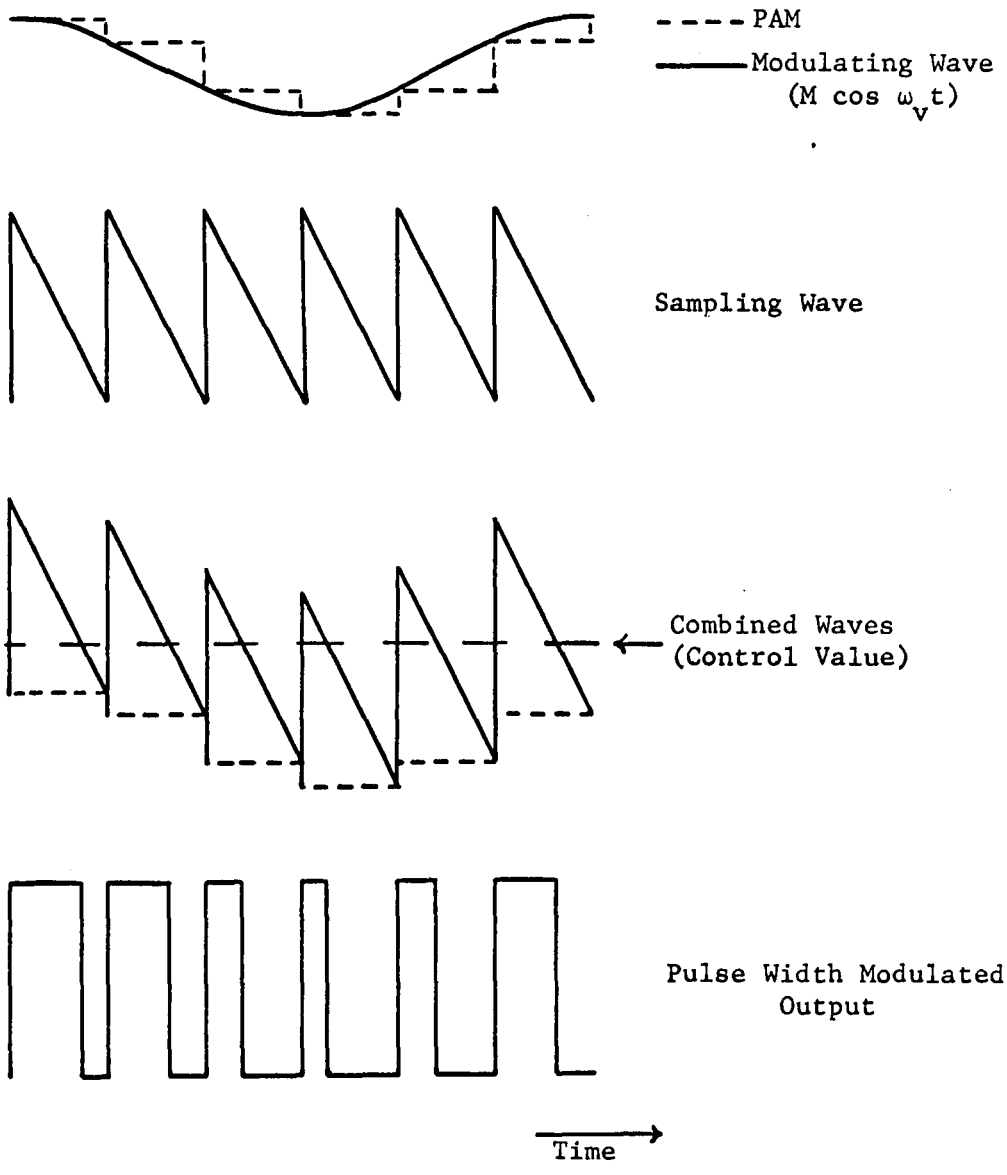

Fig. 2.1.2. Generation of PWM using uniform sampling.

$$F_4(t) = k - \sum_{n=1}^{\infty} \frac{J_n\left(\frac{n\pi M\omega_v}{\omega_c}\right)}{\frac{n\pi\omega_v}{\omega_c}} \sin\left(n\omega_v t - \frac{2n\pi k\omega_v}{\omega_c} - \frac{n\pi}{2}\right)$$

$$+ \sum_{m=1}^{\infty} \frac{1-J_o(m\pi M)}{m\pi} \sin(\omega_c t)$$

$$- \sum_{m=1}^{\infty} \sum_{n=\pm 1}^{\pm\infty} \frac{J_n\left[(m\omega_c+n\omega_v)\frac{\pi M}{\omega_c}\right]}{(m\omega_c+n\omega_v)\frac{\pi}{\omega_c}} \sin\left[(m\omega_c+n\omega_v)\left(t-\frac{2\pi k}{\omega_c}\right)-\frac{n\pi}{2}\right] \quad (2.1.6)$$

For pulses with leading edges modulated, the spectrum is of the same form as for $F_4(t)$ but with $(-t)$ substituted for t; i.e.,

$$F_5(t) = F_4(-t) \quad (2.1.7)$$

For pulses with both edges modulated (an isoceles triangle wave is used for the sampling wave) the spectrum [5] is

$$F_6(t) = F_4(t)+F_5(t)$$

$$= k_d - \sum_{n=1}^{\infty} \frac{2J_n\left(\frac{n\pi M_d \omega_v}{2\omega_c}\right)}{\frac{n\pi\omega_s}{\omega_c}} \sin(n\omega_v t) \cos\left(\frac{n\pi k_d\omega_v}{\omega_c} + \frac{n\pi}{2}\right)$$

$$- \sum_{m=1}^{\infty} \sum_{n=\pm 1}^{\pm\infty} \frac{2J_n\left[(m\omega_c+n\omega_v)\frac{\pi M_d}{2\omega_c}\right]}{(m\omega_c+n\omega_v)\frac{\pi}{\omega_c}}$$

$$\cdot \sin(m\omega_c+n\omega_v) \cos\left[(m\omega_c+n\omega_v)\frac{\pi k_d}{\omega_c} - \frac{n\pi}{2}\right] \quad (2.1.8)$$

An examination of Eqs. (2.1.6), (2.1.7) and (2.1.8) reveals the presence of harmonics of the modulating signal, in addition to sideband terms such as those present in Eqs. (2.1.1), (2.1.2) and (2.1.3). For $\omega_c=5\omega_v$, 30% modulation (M=0.3) and double-edge modulation, uniform sampling produces 1.5% sideband distortion and 30% harmonic distortion, while natural sampling produces only 0.05% sideband and no harmonic distortion [6]. Thus, natural sampling is clearly superior to uniform sampling from a distortion standpoint. In addition, production of natural sampling is much simpler since it does not require conversion to pulse-amplitude modulation.

Exact recovery of the modulation from a uniformly-sampled pulse train can be obtained by the reverse of the process by which it was made; i.e., by reconversion to pulse-amplitude modulation, followed by a low-pass filter [7]. However, this would be impossible to do in a Class D amplifier, because it is necessary for the output devices (tubes, transistors, SCR's, etc.) to be either fully "on" or fully "off".

Since uniform sampling has many disadvantages and no advantages over natural sampling when used in a Class D amplifier, natural sampling is used almost universally in this application.

2.2 New Mode Class D Amplification

The modulation used in New Mode Class D amplification is produced similarly to conventional PWM using double-edge modulation and natural sampling. However, two control values are used instead of one. This process is illustrated in Fig. 2.2.1. Whenever the combined waveforms' instantaneous voltage (Fig. 2.2.1 (c)) exceeds control value number 1, a positive output is produced. Whenever this voltage is less than

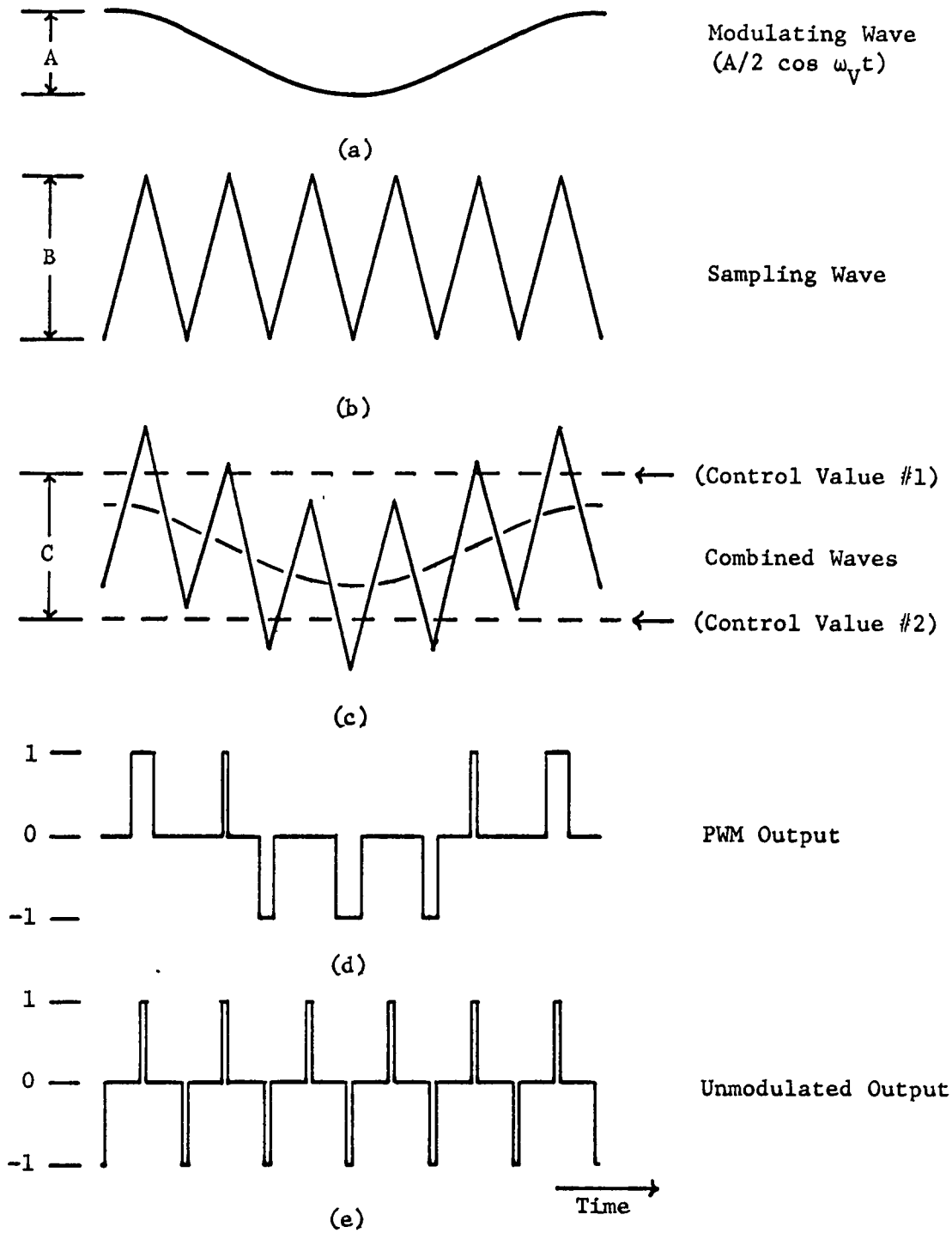

Fig. 2.2.1. Modulation process used in the New Mode of class D amplification.

control value number 2, a negative output is produced. Note that the peak-to-peak value of the sampling triangle-wave is greater than the difference between the control values (i.e., B>C). If this were not the case, a "dead band" would result; and there would be no output for inputs less than a certain value.

When no modulation is present, the output is a series of alternating positive and negative pulses. Since the control values are symmetrically spaced about the dc level of the triangle-wave, the positive and negative pulses are of equal width. For modulation levels having the peak of the modulating wave less than (B-C)/2, with B and C defined in Fig. 2.2.1, the output is simply two conventional PWM signals, one above the zero axis and one below it. Referring to Fig. 2.2.2, it is obvious that the top train of pulses is double-edge-modulated PWM, whose spectrum is given by $F_3(t)$:

$$F_3(t) = k_d + \frac{M_d}{2}\cos(\omega_v t) + 2\sum_{m=1}^{\infty}\frac{J_o(m\pi\frac{M_d}{2})}{m\pi}\sin(m\pi k_d)\cos(m\omega_c t)$$

$$+2\sum_{m=1}^{\infty}\sum_{n=\pm 1}^{\pm\infty}\frac{J_n(m\pi\frac{M_d}{2})}{m\pi}\sin(m\pi k_d + \frac{n\pi}{2})\cos(m\omega_c t + n\omega_v t) \quad (2.1.3)$$

where $k_d = a/b$ and $M_d = A/(B-C)$, referring to Fig. 2.2.1. As the pulses of the top train are becoming larger, those of the bottom train are becoming smaller and vice versa; i.e., the sense (phase) of the modulation is reversed on the lower train. Also, the carrier on the lower train is shifted by π from that of the upper. Thus, by shifting the phase of both the carrier and the modulation of $F_3(t)$ by π radians, we

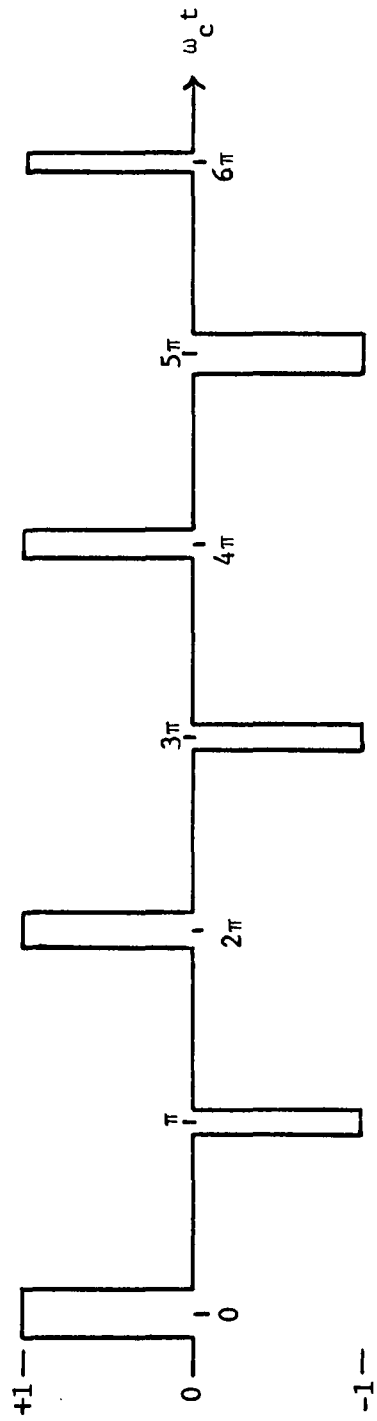

Fig. 2.2.2. New Mode modulation output for very low modulation level.

develop an expression for what the lower pulse train would be if it consisted of positive pulses. This expression is

$$F_7(\omega_v t, \omega_c t) = F_3(\omega_v t+\pi, \omega_c t+\pi)$$

$$= k_d - \frac{M_d}{2} \cos(\omega_v t)$$

$$+2 \sum_{m=1}^{\infty} \frac{(-1)^m J_o(m\pi \frac{M_d}{2})}{m\pi} \sin(m\pi k_d) \cos(m\omega_c t)$$

$$+2 \sum_{m=1}^{\infty} \sum_{n=\pm 1}^{\pm\infty} \frac{(-1)^{m+n} J_n(m\pi \frac{M_d}{2})}{m\pi} \sin(m k_d + \frac{n\pi}{2}) \cos(m\omega_c t + n\omega_v t) \quad (2.2.1)$$

The expression for the combined pulse trains is the difference between $F_3(t)$ and $F_7(t)$, which is

$$F_8(t) = F_3(t) - F_7(t)$$

$$= M_d \cos(\omega_v t) + 2 \sum_{m=1}^{\infty} [1-(-1)^m] \frac{J_o(m\pi \frac{M_d}{2})}{m\pi} \sin(m\pi k_d) \cos(m\omega_c t)$$

$$+2 \sum_{m=1}^{\infty} \sum_{n=\pm 1}^{\pm\infty} [1-(-1)^{m+n}] \frac{J_n(m\pi \frac{M_d}{2})}{m\pi} \sin(m\omega k_d + \frac{n\pi}{2}) \cos(m\omega_c t + n\omega_v t) \quad (2.2.2)$$

In the limiting case of $k_d=1/2$, which corresponds to C=0 in Fig. 2.2.1, the waveform is identical in form to a conventional pulse-width modulated wave with $k_d=1/2$; i.e., the trailing edges of the upper train coincide with the leading edges of the lower and vice versa. Substituting $k_d=1/2$ into the expressions for $F_8(t)$ (combined pulse trains) and $F_3(t)$, we see that $F_8(t)$ becomes twice $F_3(t)$ without the dc term. This is obvious because $F_8(t)$ is made up of pulses of both

polarities whose average values cancel. Note that, with $k_d=1/2$, the even harmonic terms of both F_3 and F_8 are zero, but for $k_d<1/2$, these terms are zero only in F_8.

If, during the modulation cycle, any pulses disappear (i.e., A>B-C, referring to Fig. 2.2.1), the output becomes much more difficult to analyze. Following the method outlined by Black [8], we imagine an endless series of walls in the xy plane. All walls rest on the xy plane and are of unit height in the z direction. All walls have identical shape. To analyze a PWM system with trailing edge modulated, we make the left edge of the wall straight and make the right edge conform to the shape of the desired modulation. For the case of natural sampling, a plane is passed through the z axis as shown in Fig. 2.2.3. The intersection of the walls with this plane is projected onto the xz plane. The result is a pulse-width-modulated wave with trailing edge modulation and natural sampling.

Consider the upper pulse train of Fig. 2.2.2. Consider only the right "half" of each pulse (i.e., that portion from 0, 2π, 4π, etc., to the end of the pulse). This becomes a train of naturally-sampled, trailing-edge-modulated pulses when modulation is applied. By giving the walls in Fig. 2.2.3 the shape shown, the xz plane projection is the above train of pulses, provided we substitute:

$$x = \omega_c t \tag{2.2.3}$$

and

$$y = \omega_v t \tag{2.2.4}$$

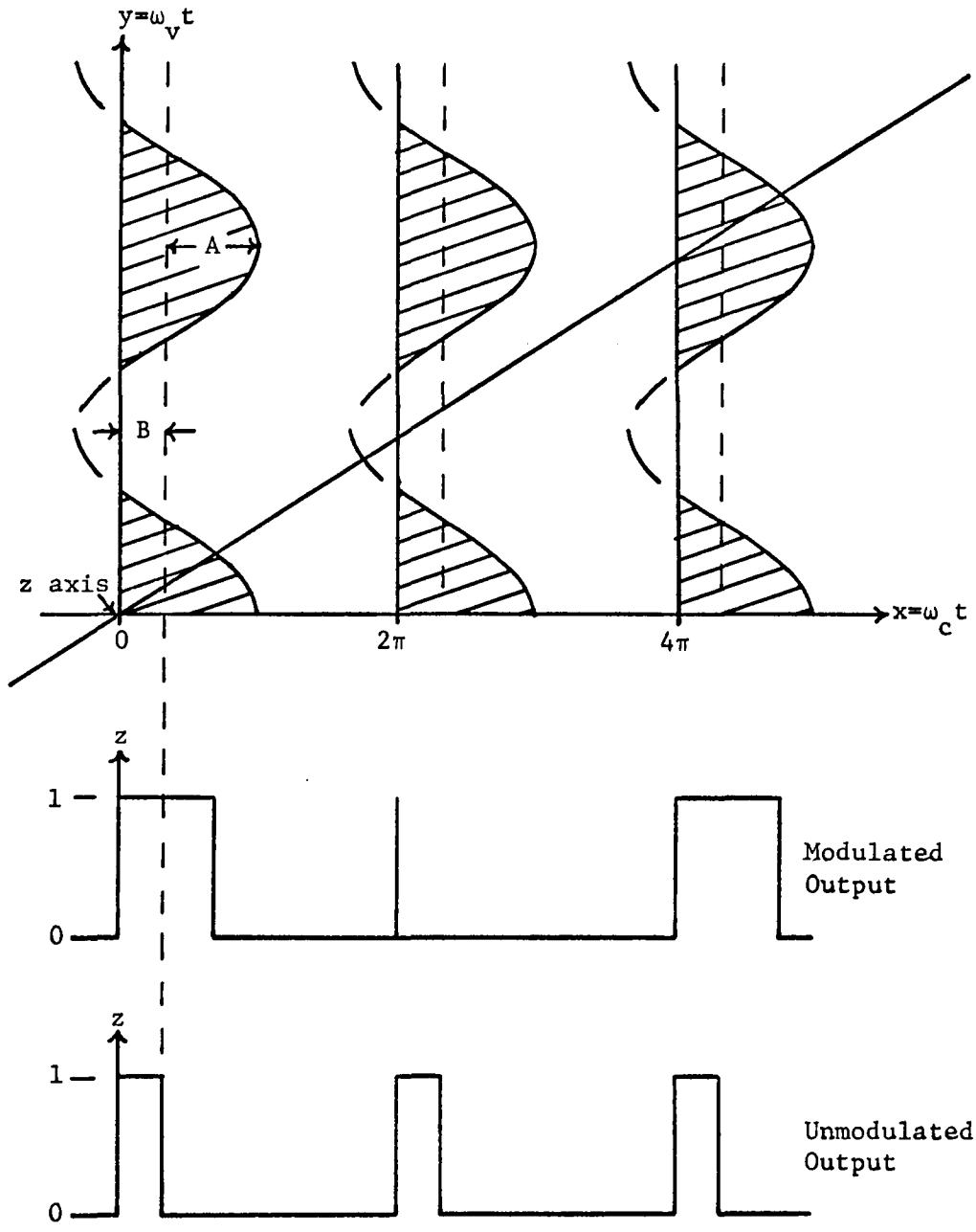

Fig. 2.2.3. Graphical representation of New Mode modulation process.

The equation of the "first" wall's right surface, from y = 0 to 2, is

$$x = B + A \cos y \qquad 0 \leq y \leq \theta \qquad (2.2.5)$$

$$x = 0 \qquad \theta \leq y \leq 2\pi - \theta$$

$$x = B + A \cos y \qquad 2\pi - \theta \leq y \leq 2\pi$$

where $\theta = \cos^{-1}(-\frac{B}{A})$ (Note that the A and B of this analysis are different from the A and B of Fig. 2.2.1). The equation of the plane is

$$x = (\omega_c/\omega_v)\, y \qquad (2.2.6)$$

We now define two constants which are functions of the pulse train, k and M. The first of these, k, is the ratio of pulse width to the interval between pulse centers for unmodulated pulses. That is:

$$k = \frac{B}{2\pi} \qquad (2.2.7)$$

The second of these constants, M, is the Modulation Index. It is the excursion of the modulated edge divided by the maximum allowable excursion of 2π. The excursion of the modulated edge is 2A for $A \leq B$. The excursion for $A \geq B$ is A+B. Thus, we could have two modulation indexes, one for low modulation levels equal to A/π, and one for high modulation levels equal to $(A+B)/2\pi$. However, for convenience we shall let

$$M = \frac{A}{\pi} \qquad (2.2.8)$$

Black [9] has shown that the modulated pulse train of Fig. 2.2.3 can be expressed by the double Fourier series:

$$F(x,y) = 1/2\ A_{oo} + \sum_{n=1}^{\infty} [A_{on} \cos(ny) + B_{on} \sin(ny)]$$

$$+ \sum_{m=1}^{\infty} [A_{mo} \cos(mx) + B_{mo} \sin(mx)]$$

$$+ \sum_{m=1}^{\infty} \sum_{n=\pm 1}^{\pm\infty} [A_{mn} \cos(mx+ny) + B_{mn} \sin(mx+ny)] \qquad (2.2.9)$$

where

$$A_{mn} = \frac{1}{2\pi^2} \int_0^{2\pi} \int_0^{2\pi} F(x,y) \cos(mx+ny)\, dxdy \qquad (2.2.10)$$

and

$$B_{mn} = \frac{1}{2\pi^2} \int_0^{2\pi} \int_0^{2\pi} F(x,y) \sin(mx+ny)\, dxdy \qquad (2.2.11)$$

The coefficients A_{mn} and B_{mn} can be combined in the complex form:

$$A_{mn} + i\, B_{mn} = \frac{1}{2\pi^2} \int_0^{2\pi} \int_0^{2\pi} F(x,y) e^{i(mx+ny)}\, dxdy \qquad (2.2.12)$$

F(x,y) has only two values, 0 and 1. For values of y from 0 to θ and from $2\pi-\theta$ to 2π,

$$F(x,y) = 1 \qquad 0 < x < B + A \cos y$$

$$F(x,y) = 0 \qquad B + A \cos y < x < 2\pi \qquad (2.2.13)$$

For values of y between θ and $2\pi-\theta$, F(x,y) = 0. With this information Eq. (2.2.12) becomes:

$$A_{mn} + i\, B_{mn} = \frac{1}{2\pi^2}\int_0^{\theta}\int_0^{B+A\cos y} e^{i(mx+ny)}\,dx\,dy$$

$$+ \frac{1}{2\pi^2}\int_{2\pi-\theta}^{2\pi}\int_0^{B+A\cos y} e^{i(mx+ny)}\,dx\,dy \qquad (2.2.14)$$

This can be written:

$$A_{mn} + i\, B_{mn} = \frac{1}{2\pi^2}\int_0^{2\pi}\int_0^{B+A\cos y} e^{i(mx+ny)}\,dx\,dy$$

$$- \frac{1}{2\pi^2}\int_{\theta}^{2\pi-\theta}\int_{\theta}^{B+A\cos y} e^{i(mx+ny)}\,dx\,dy \qquad (2.2.15)$$

Integrating with respect to x, we get:

$$A_{mn} + i\, B_{mn} = \frac{-i}{2\pi^2 m}\int_0^{2\pi} e^{imB+imA\cos y+iny}\,dy$$

$$+ \frac{i}{2\pi^2 m}\int_0^{2\pi} e^{iny}\,dy + \frac{i}{2\pi^2 m}\int_{\theta}^{2\pi-\theta} e^{imB+imA\cos y+iny}\,dy$$

$$- \frac{i}{2\pi^2 m}\int_{\theta}^{2\pi-\theta} e^{iny}\,dy \qquad (2.2.16)$$

We rewrite the third integral in Eq. (2.2.16) as

$$I_3 = e^{imB} \int_{\theta}^{2\pi-\theta} e^{imA \cos y} e^{iny} dy \qquad (2.2.17)$$

This is not integrable in this form. We can express exp (imA cos y) in a Fourier series with Bessel coefficients [10]:

$$e^{imA \cos y} = J_o(mA) + 2i \cos y \, J_1(mA) + 2i^2 \cos (2y) \, J_2(mA)$$

$$+ 2i^3 \cos(3y) J_3(mA) + \ldots$$

$$= J_o(mA) + \sum_{p=1}^{\infty} 2i^p \cos (py) \, J_p(mA) \qquad (2.2.18)$$

Substituting this into Eq. (2.2.17) and integrating term by term, we get:

$$I_3 = -\frac{2e^{imB} - J_o(mA)}{n} \sin (n\theta)$$

$$+ \sum_{\substack{p=1 \\ p \neq \pm n}}^{\infty} \frac{4e^{imB} J_p(mA)}{p^2 - n^2} [n \sin (n\theta) \cos (p\theta) - p \cos (n\theta) \sin (p\theta)]$$

$$+ \frac{2e^{imB} i^n J_n(mA)}{n} [n\pi - n\theta - \cos (n\theta) \sin (n\theta)] \qquad (2.2.19)$$

To evaluate the first integral in Eq. (2.2.16) we merely substitute $\theta=0$ into Eq. (2.2.19):

$$I_1 = 2\pi \, i^n J_n(mA) e^{imB} \qquad (2.2.20)$$

The fourth integral in Eq. (2.2.16) evaluates out to be:

$$I_4 = -\frac{2}{n}\sin(n\theta) \tag{2.2.21}$$

By setting $\theta = 0$ in Eq. (2.2.21) we obtain zero for the value of the second integral of Eq. (2.2.16). Substituting Eqs. (2.2.19) through (2.2.21) into Eq. (2.2.16) and collecting terms, we get:

$$\begin{aligned} A_{mn}+iB_{mn} = {} & \frac{ie^{imB}i^n J_n(mA)}{\pi^2 mn}\,[-n\theta - \cos(n\theta)\sin(n\theta)] \\ & - \frac{ie^{imB}J_o(mA)}{\pi^2 mn}\sin(n\theta) \\ & + \sum_{\substack{p=1 \\ p\neq\pm n}}^{\infty} \frac{2ie^{imB}i^p J_p(mA)}{\pi^2 m(p^2-n^2)}\,[n\sin(n\theta)\cos(p\theta) - p\cos(n\theta)\sin(p\theta)] \\ & + \frac{i\sin(n\theta)}{\pi^2 mn} \end{aligned} \tag{2.2.22}$$

Substituting $\exp\left(\frac{in\pi}{2}\right)$ and $\exp\left(\frac{ip\pi}{2}\right)$ for i^n and i^p, respectively, in Eq. (2.2.22), and solving for real and imaginary parts, we get:

$$\begin{aligned} A_{mn} = {} & \frac{\sin(mB+\frac{n\pi}{2})J_n(mA)}{\pi^2 mn}\,[n\theta + \cos(n\theta)\sin(n\theta)] \\ & + \frac{\sin(mB)J_o(mA)}{\pi^2 mn}\sin(n\theta) \\ & - \sum_{\substack{p=1 \\ p\neq\pm n}}^{\infty} \frac{2\sin(mB+\frac{p\pi}{2})J_p(mA)}{\pi^2 m(p^2-n^2)}\,[n\sin(n\theta)\cos(p\theta) - p\cos(n\theta)\sin(p\theta)] \end{aligned} \tag{2.2.23}$$

and

$$B_{mn} = \frac{\cos(mB+\frac{n\pi}{2})J_n(mA)}{\pi^2 mn}[-n\theta - \cos(n\theta)\sin(n\theta)]$$

$$- \frac{\cos(mB)J_o(mA)}{\pi^2 mn}\sin(n\theta)$$

$$+ \sum_{\substack{p=1 \\ p\neq\pm n}}^{\infty} \frac{2\cos(mB+\frac{p\pi}{2})J_p(mA)}{\pi^2 m(p^2-n^2)}[n\sin(n\theta)\cos(p\theta) - p\cos(n\theta)\sin(p\theta)]$$

$$+ \frac{\sin(n\theta)}{\pi^2 mn} \qquad (2.2.24)$$

The above equations are invalid for m=0 and n=0. Going back to Eq. (2.2.15), we solve for the remaining coefficients in Eq. (2.2.9):

$$A_{oo} = \frac{B\theta}{\pi^2} \qquad (2.2.25)$$

$$A_{o1} = \frac{B}{\pi^2}\sin\theta - \frac{A}{2\pi^2}\sin\theta\cos\theta + \frac{A\theta}{2\pi^2} \qquad (2.2.26)$$

$$A_{on}(n\neq 1) = \frac{B}{\pi^2 n}\sin(n\theta)$$

$$+ \frac{A}{\pi^2(1-n^2)}[\cos(n\theta)\sin\theta - n\sin(n\theta)\cos\theta] \qquad (2.2.27)$$

$$B_{on} = 0 \qquad (2.2.28)$$

$$A_{mo} = \frac{\theta J_o(mA)}{\pi^2 m}\sin(mB) + \sum_{p=1}^{\infty} \frac{2\sin(mB+\frac{p\pi}{2})J_p(mA)\sin(p\theta)}{\pi^2 mp} \qquad (2.2.29)$$

$$B_{mo} = \frac{\theta}{\pi^2 m} - \frac{\theta J_o(mA)}{\pi^2 m}\cos(mB) - \sum_{p=1}^{\infty} \frac{2\cos(mB+\frac{p\pi}{2})J_p(mA)\sin(p\theta)}{\pi^2 mp} \qquad (2.2.30)$$

Substituting Eqs. (2.2.3), (2.2.4), (2.2.7) and (2.2.8) into Eqs. (2.2.23) through (2.2.30) and substituting these latter into Eq. (2.2.9) and simplifying, we obtain:

$$F_9(t) = \frac{k\theta}{\pi} + [\frac{2k}{\pi}\sin\theta - \frac{M}{4\pi}\sin(2\theta) + \frac{M\theta}{2\pi}]\cos(\omega_v t)$$

$$+ \sum_{n=2}^{\infty} [\frac{2k\sin(n\theta)}{\pi n} + \frac{M[(1-n)\sin(\theta+n\theta)+(1+n)\sin(\theta-n\theta)]}{2\pi(1-n^2)}]\cos(n\omega_v t)$$

$$+ \sum_{m=1}^{\infty} \frac{\theta}{\pi^2 m}\sin(m\omega_c t) - \sum_{m=1}^{\infty} \frac{\theta J_o(m\pi M)}{\pi^2 m}\sin(m\omega_c t - 2m\pi k)$$

$$- \sum_{m=1}^{\infty}\sum_{p=1}^{\infty} \frac{2J_p(m\pi M)\sin(p\theta)}{\pi^2 mp}\sin(m\omega_c t - 2m\pi k - \frac{p\pi}{2})$$

$$+ \sum_{m=1}^{\infty}\sum_{n=\pm 1}^{\pm\infty} \frac{1}{\pi^2 mn}\sin(n\theta)\sin(m\omega_c t + n\omega_v t)$$

$$- \sum_{m=1}^{\infty}\sum_{n=\pm 1}^{\pm\infty} \frac{1}{\pi^2 mn}\sin(n\theta)J_o(m\pi M)\sin(m\omega_c t + n\omega_v t - 2m\pi k)$$

$$- \sum_{m=1}^{\infty}\sum_{n=\pm 1}^{\pm\infty} \frac{1}{2\pi^2 mn}[2n\theta + \sin(2n\theta)]J_n(m\pi M)\sin(m\omega_c t + n\omega_v t - 2m\pi k - \frac{n\pi}{2})$$

$$+ \sum_{m=1}^{\infty}\sum_{n=\pm 1}^{\pm\infty}\sum_{\substack{p=1 \\ p\neq\pm n}}^{\infty} \frac{J_p(m\pi M)}{\pi^2 m(p^2-n^2)}[(n-p)\sin(n\theta+p\theta)+(n+p)\sin(n\theta-p\theta)]$$

$$\cdot\sin(m\omega_c t + n\omega_v t - 2m\pi k - \frac{n\pi}{2}) \qquad (2.2.31)$$

where

$$\theta = \cos^{-1}\left(\frac{-2k}{M}\right);\ 0 \le \theta \le \pi \tag{2.2.32}$$

Substituting $\theta=\pi$ in Eq. (2.2.31), we obtain the series for conventional PWM with trailing edge modulated; that is, $F_1(t)$ of Eq. (2.1.1).

Equation (2.2.31) is the series for the right halves of the upper pulse train of Fig. 2.2.1. To obtain the expression for the left halves (leading edges modulated), we merely reverse the time scale of Eq. (2.2.34); i.e.,

$$F_{10}(t) = F_9(-t) \tag{2.2.33}$$

The expression for the entire upper pulse train is

$$F_{11}(t) = F_9(t)+F_{10}(t) \tag{2.2.34}$$

As was the case for lower modulation levels, we obtain the expression for the lower pulse train by shifting the phase of both the carrier and the modulation by π. Thus,

$$F_{12}(\omega_c t,\omega_v t) = F_{11}(\omega_c t+\pi,\omega_v t+\pi) \tag{2.2.35}$$

The expression for the combined pulse trains is the difference of the two:

$$F_{13}(t) = F_{11}(t) - F_{12}(t)$$

$$= \left[\frac{4k_d}{\pi} \sin\theta - \frac{M_d}{2\pi}\sin(2\theta) + \frac{M_d\theta}{\pi}\right] \cos(\omega_v t)$$

$$+ \sum_{\substack{n=3 \\ n \text{ odd}}}^{\infty} \left[\frac{4k_d \sin(n\theta)}{\pi n} + \frac{M_d[(1-n)\sin(\theta+n\theta)+(1+n)\sin(\theta-n\theta)]}{\pi(1-n^2)}\right] \cos(m\omega_v t)$$

$$+ \sum_{\substack{m=1 \\ m \text{ odd}}}^{\infty} \frac{4\theta J_o(\frac{m\pi M_d}{2})}{\pi^2 m} \cos(m\omega_c t) \sin(m\pi k_d)$$

$$+ \sum_{\substack{m=1 \\ m \text{ odd}}}^{\infty} \sum_{p=1}^{\infty} \frac{8J_p(\frac{m\pi M_d}{2}) \sin(p\theta)}{\pi^2 mp} \cos(m\omega_c t) \sin(m\pi k_d + \frac{p\pi}{2})$$

$$+ \sum_{\substack{m=1 \\ (m+n)\text{odd}}}^{\infty} \sum_{n=\pm 1}^{\pm\infty} \frac{4\sin(n\theta)}{\pi^2 mn} J_o(\frac{m\pi M_d}{2}) \cos(m\omega_c t + n\omega_v t) \sin(m\pi k_d)$$

$$+ \sum_{\substack{m=1 \\ (m+n)\text{odd}}}^{\infty} \sum_{n=\pm 1}^{\pm\infty} \frac{2}{\pi^2 mn} [2n\theta + \sin(2n\theta)] J_n(\frac{m\pi M_d}{2}) \cos(m\omega_c t + n\omega_v t) \sin(m\pi k_d + \frac{n\pi}{2})$$

$$- \sum_{\substack{m=1 \\ (m+n)\text{odd}}}^{\infty} \sum_{n=\pm 1}^{\pm\infty} \sum_{\substack{p=1 \\ p\neq\pm n}}^{\infty} \frac{4J_p(\frac{m\pi M_d}{2})}{\pi^2 m(p^2-n^2)} [(n-p)\sin(n\theta+p\theta)+(n+p)\sin(n\theta-p\theta)]$$

$$\cdot \cos(m\omega_c t + n\omega_v t) \sin(m\pi k_d + \frac{n\pi}{2}), \qquad (2.2.36)$$

where

$$k_d = 2k \qquad (2.2.37)$$

and

$$M_d = 2M. \tag{2.2.38}$$

Note that most of the even harmonics present in Eq. (2.2.31) are absent from Eq. (2.2.36). Thus we have an expression for the output of New Mode PWM. Let us now examine the relationship between k_d, M_d and θ.

The unmodulated duty cycle k_d of the upper or lower train of pulses is a property of the system and it usually ranges from 0 to about 0.2. Given that k_d is constant, θ is a clear function of the modulation level M_d (see Eq. (2.2.32)). As M_d is reduced (for positive values of k_d), θ approaches π, and finally a level of M_d is found for which $\theta = \pi$. For values of M_d below this level, θ becomes complex with its real part still equal to π. If $\theta = \pi$ is substituted into Eq. (2.2.36), this equation reduces to Eq. (2.2.2).

For small positive or negative values of k_d, as M_d is increased, θ approaches $\pi/2$. If k_d is zero, then $\theta = \pi/2$ for all modulation levels. If $\theta = \pi/2$, no pulses would appear at all unless some modulation was present. Substituting $\theta = \pi/2$ and $k_d = 0$ into Eq. (2.2.36), we obtain

$$F_{14}(t) = \frac{M_d}{2}\cos(\omega_v t) + \sum_{\substack{m=1\\ m\ \text{odd}}}^{\infty}\sum_{\substack{p=1\\ p\ \text{odd}}}^{\infty}\frac{8J_p\left(\frac{m\pi M_d}{2}\right)}{\pi^2 mp}\cos(m\omega_c t)$$
$$+2\sum_{\substack{m=2\\ m\ \text{even}}}^{\infty}\sum_{\substack{n=\pm 1\\ n\ \text{odd}}}^{\pm\infty}\frac{2(-1)^{\frac{n-1}{2}}}{\pi m}J_n\left(\frac{m\pi M_d}{2}\right)\cos(m\omega_c t+n\omega_v t)$$
$$-\sum_{\substack{m=2\\ m\ \text{even}}}^{\infty}\sum_{\substack{n=\pm 1\\ n\ \text{odd}}}^{\pm\infty}\sum_{\substack{p=2\\ p\ \text{even}}}^{\infty}\frac{8n(-1)^{\frac{p}{2}}J_p\left(\frac{m\pi M_d}{2}\right)}{\pi^2 m(p^2-n^2)}\cos(m\omega_c t+n\omega_v t) \tag{2.2.39}$$

What a simplification! Three whole summations are eliminated as well as half of the terms of the remaining double summations and three fourths of the terms of the remaining triple summation. In addition there are no harmonics of the modulating frequency present. Let us compare this "ideal" New Mode output with conventional PWM using double-edge modulation and natural sampling.

Usually in a conventional Class D amplifier, a 50% duty cycle is used, so we will assume $k_d=1/2$. Substituting this into Eq. (2.1.3), we obtain:

$$F_3(t) = 1/2+ \frac{M_d}{2} \cos(\omega_v t) - \sum_{\substack{m=1 \\ m \text{ odd}}}^{\infty} \frac{(-1)^{\frac{m-1}{2}} 2J_o(m\pi\frac{M_d}{2})}{m\pi}$$

$$- \sum_{m=1}^{\infty} \sum_{\substack{n=\pm 1 \\ (m+n)\text{odd}}}^{\pm\infty} \frac{(-1)^{\frac{m+n-1}{2}} 2J_n(m\pi\frac{M_d}{2})}{m\pi} \cos(m\omega_c t+n\omega_v t) \qquad (2.2.40)$$

We wish to compare the distortion performance of the two systems. The only terms of Eqs. (2.2.39) and (2.2.40) that represent distortion are those containing $\cos(m\omega_c t+n\omega_v t)$. (Distortion is defined as the sum of all outputs, other than dc or the desired modulation, which occur within the band of frequencies the amplifier was designed to amplify).

The coefficient of $\cos(m\omega_c t+n\omega_v t)$ for conventional PWM (Eq. (2.2.40)) is:

$$- \frac{(-1)^{\frac{m+n-1}{2}} 2J_n(m\pi\frac{M_d}{2})}{m\pi} \qquad (2.2.41)$$

The coefficient of $\cos(m\omega_c t+n\omega_v t)$ for New Mode is:

$$\frac{(-1)^{\frac{n-1}{2}}\, 2J_n\left(m\pi\frac{M_d}{2}\right)}{m\pi} - \sum_{\substack{p=2 \\ p \text{ even}}}^{\infty} \frac{8n(-1)^{\frac{p}{2}} J_p\left(m\pi\frac{M_d}{2}\right)}{m\pi^2(p^2-n^2)} \qquad (2.2.42)$$

The first term of (2.2.42) is equal in absolute value to expression (2.2.41). The largest (absolute value) term of the summation in (2.2.42) occurs when p and n differ by 1 (p is always even and n is always odd, so they are never equal). Even then,

$$\frac{2}{m\pi} \gtrsim \left|\frac{8n}{m\pi^2(p^2-n^2)}\right| \qquad (2.2.43)$$

for all allowable values of p. The summation in (2.2.42) converges rapidly and has as many negative terms as it does positive ones. Thus it can be easily seen that, on the average, the absolute value of (2.2.42) will not be much different than that of (2.2.41). However, there is one important difference. Only half as many values of m and n are allowable in expression (2.2.42)! In (2.2.41), the sum of m and n must be odd. But in (2.2.42), in addition to this restriction, m must be even, and therefore n must always be odd.

Thus it appears that new Mode Class D amplification is somewhat superior to conventional Class D amplification from a distortion standpoint, provided that $\theta = \pi/2$. The only way for θ to be close to $\pi/2$ for all modulation levels is for k_d to equal zero. In any real system, k_d can not be set exactly to zero. If k_d is slightly positive, as M_d is reduced, θ will approach (and reach) π; and the output at modulation frequency will be twice the proper value. Compare Eq. (2.2.2) with

Eq. (2.2.39). If k_d is slightly negative, then as M_d is reduced, θ will approach zero; and the output of the system will be zero. Thus we have a choice: either zero output at very low levels of modulation or twice normal output at very low levels. The latter seems far less objectionable and is more correctable with negative feedback, so k_d is usually set to some small positive value to insure that, with component variations, etc., k_d never becomes negative.

In practical New Mode Class D systems such deficiencies as rounding of the corners of the triangle (or sawtooth) modulating wave, reduction in amplitude of narrower pulses due to slow switching speeds, etc., cause additional distortion at the crossover points (crossover points occur when $\frac{M_d}{2} \cos(\omega_v t) = k_d$). However, by careful circuit design these effects can be minimized and a New Mode Class D amplifier can have distortion performance comparable to a conventional Class D amplifier without any increase in switching frequency.

CHAPTER III

AN AMPLIFIER USING THE NEW MODE

An amplifier which can be operated in either the conventional mode or the New Mode is described in this chapter. A complete circuit description is given, including an analysis of the characteristics of the output filter when the amplifier is operated in the New Mode.

3.1 System Description

A block diagram of the amplifier is shown in Fig. 3.1.1. Since this amplifier was designed for study of a principle rather than for application, a rather complex fixed-frequency, non-self-oscillating design was chosen. This is in contrast to the much simpler self-oscillating (feedback type) designs of Johnson [11] and Turnbull and Townsend [12] for conventional Class D amplifiers.

Since this amplifier uses double edge modulation, a triangle-wave is used as the sampling wave. It is produced by passing the output of a 100 KHz oscillator through a slicer to produce a square wave, and by passing this square wave through a Miller integrator.

Natural sampling is used in this bi-modal amplifier, so the modulating signal (audio) is added linearly to the sampling wave. This is accomplished by amplifying the audio and feeding it, along with the sampling triangle-wave, into a summing amplifier. The output of this summing amplifier is fed into a bi-level slicer. When the instantaneous input to this slicer exceeds threshold no. 1 (see point F, Fig. 3.1.1), a positive output is produced. When the input is less than threshold no. 2, a negative output is produced. No output is produced for inputs

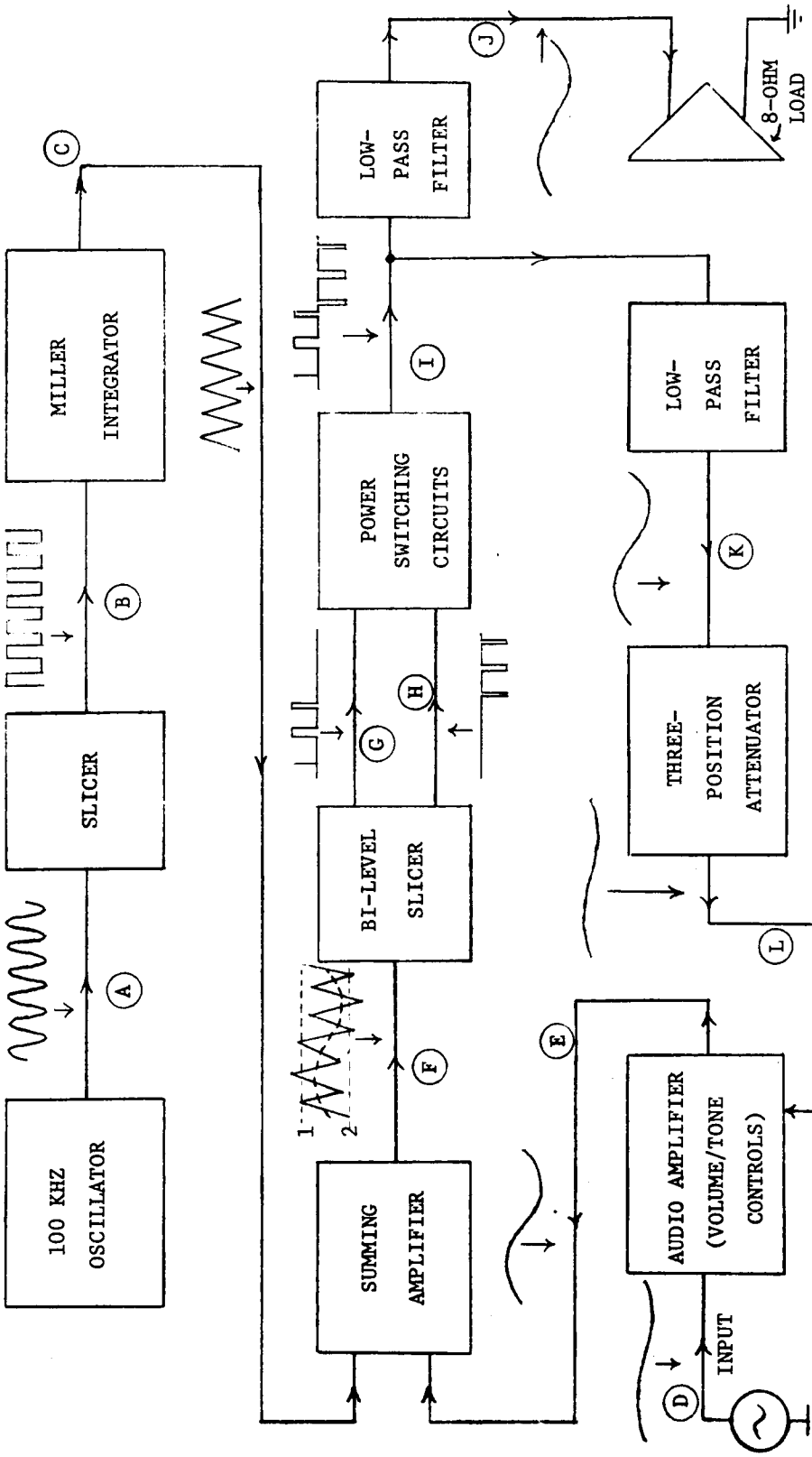

Fig. 3.1.1. Block diagram of New Mode amplifier.

between the two thresholds.

The outputs of the bi-level slicer are amplified and combined in the power switching circuit. The output of this circuit is the desired pulse-width modulation. This is fed into a low pass filter to recover the original modulation, and then to the load. This output, point (I), is also fed through another low pass filter back to the audio amplifier to provide negative feedback. There are three reasons for using separate filters:

1. Greater attenuation of switching frequencies is necessary in the feedback filter, requiring a more complex and, therefore, more lossy filter.

2. Changes in load impedance, which affect the characteristics of the output filter, should not cause instability in the feedback loop.

3. The gain vs. phase characteristics of the feedback filter must be optimized according to stability criteria.

This amplifier may be operated as a conventional Class D amplifier with a k_d of 1/2, or as a New Mode amplifier with a k_d of any value from 0 to 1/2, simply by changing the difference between the two thresholds of the bi-level slicer. If this difference is made zero, the amplifier will operate in the conventional mode. (Compare Fig. 2.2.1, with C = 0, to Fig. 2.1.1.). However, in order to compensate for the fact that the transistors in the following stages switch on faster than they switch off, C (Fig. 2.2.1.) is set at some small positive value when in the conventional mode. If this were not done, very high dissipation in the output transistors would result. Referring to Fig. 2.2.1 (e), $k_d = \frac{a}{b}$ which, by simular triangles, is also equal to

$$k_d = \frac{B - C}{2B} \qquad (3.1.1)$$

where B is the triangle-wave amplitude. This formula is correct if the difference in switching times of the output transistors is neglected.

3.2 Circuit Description[1]

The 100 KHz oscillator is a conventional twin-tee oscillator with a three-stage amplifier. The amplifier consists of an input emitter follower (Q_1), a gain stage (Q_2) and an output emitter follower (Q_3). The three stages are direct coupled, and bias for all three stages is provided by feedback from Q_3 through the twin tee. Resistors R_1 and R_2 form a voltage divider with the parallel combination of R_5 and R_6, thereby determining the ratio of quiescent Q_3 emitter voltage to Q_1 base voltage. Since Q_1 base voltage is necessarily equal to two base-emitter voltage drops, about 1.2 volts, the quiescent level at point A is simply determined. Fine adjustment of this level, necessary for proper operation of the following stage, is done by selecting R_5. Signal amplitude limiting occurs by gentle saturation of Q_2. Resistor R_4 is selected to set the loop gain of the oscillator to slightly over unity.

The slicer is simply a two-stage direct-coupled common-emitter amplifier. The turn-on voltage of Q_4 is equal to one base-emitter drop plus three diode drops, or about 2.4 volts. If the dc voltage at point A is set equal to this threshold voltage by adjusting R_5, then Q_4 will be on for half of the time and off for half of the time, resulting in a symmetrical square wave at point B. Since both the dc level at point A

---

[1] Design equations are omitted from this section for brevity. See Appendix A for approximate design equations.

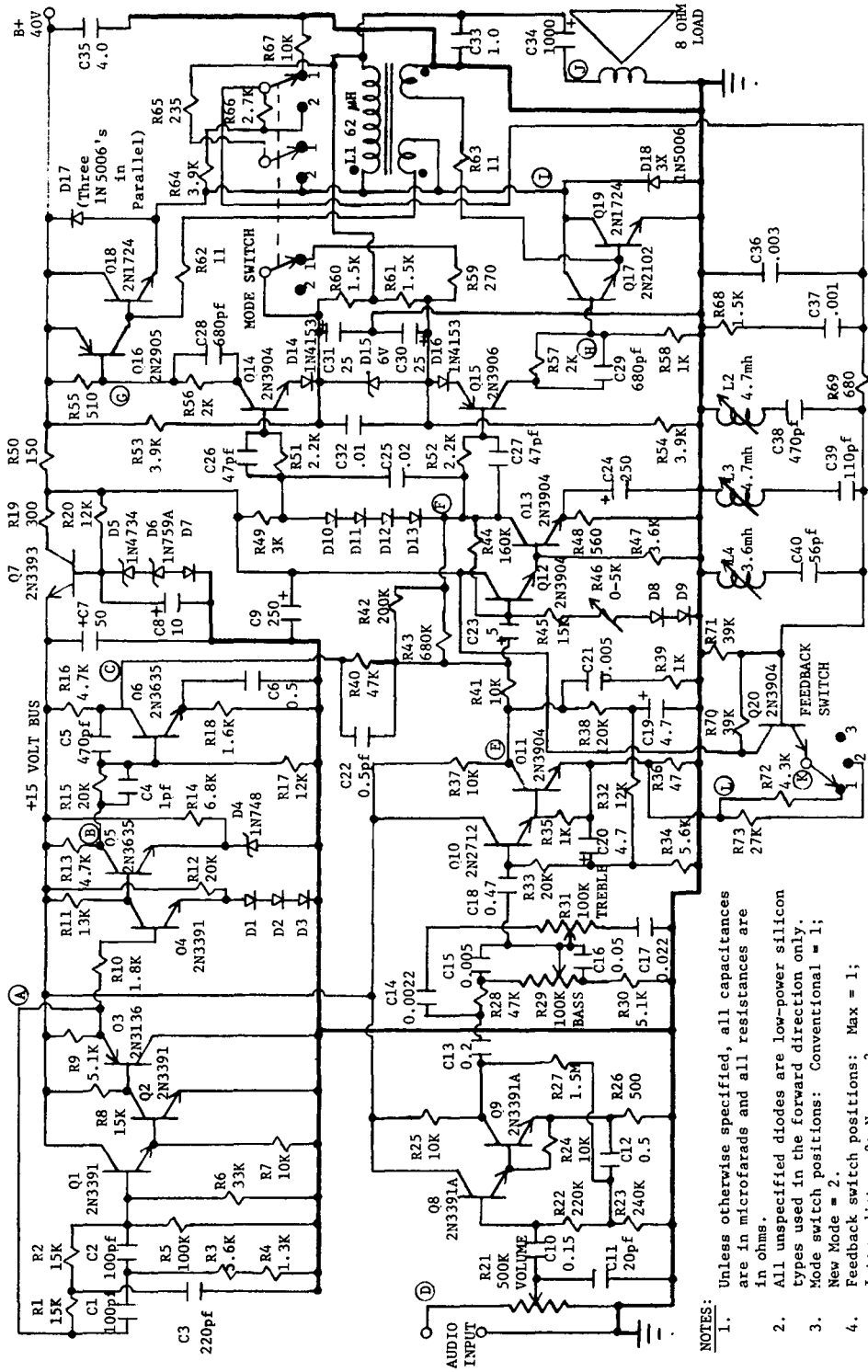

Fig. 3.2.1. Electrical schematic of New Mode amplifier.

and the slicer threshold are multiples of silicon P-N junction drops, the symmetry of the output square wave is relatively independent of changes in temperature or supply voltage. (Actually, the square wave is set considerably asymmetrical to compensate for differences in turn-off times between the two halves of the output circuit. This is only important when operating in the conventional mode.) The emitter of Q_5 is biased at one or two volts above that of Q_4 by D_4 and R_{14}. Transistor Q_5 is a high-frequency unit to insure low rise and fall times on the slicer output square wave at point B.

The square wave is fed into the Miller integrator to be converted into a triangle-wave. Transistor Q_6 serves as an operational amplifier, with C_5 as the integrating capacitor. The integrating resistor is R_{15} when Q_5 is on, and $R_{14} + R_{15}$ when Q_5 is off. This difference in integrating resistances produces a slight dc offset at the output of the integrator. The effective integrating resistance is the average of these two values. Capacitor C_4 is a high-frequency bypass designed to sharpen the peaks of the triangle-wave.

The modulating audio signal is fed into the volume control at point D. Capacitor C_{11} is a high-frequency bypass to keep frequencies above 20 KHz which may be present at the input from beating with the switching signal and producing spurious outputs. Emitter follower Q_8 presents a high impedance to the input and a low impedance to Q_9. Transistor Q_9 is a common-emitter stage with a gain of 20. Bias for both stages is supplied by R_{27}, R_{23} and R_{22}. Capacitor C_{12} "bootstraps" R_{22} to reduce its loading effect on the base of Q_8.

The output of Q_9 is fed through a standard tone control network into the second audio amplifier. This circuit is basically the same as the first, except for a much higher (open loop) gain. The input emitter-follower, Q_{10}, is biased at a much higher current than Q_8, to present a very low impedance to Q_{11} and minimize its high-frequency phase shift. Negative feedback for the entire system is applied to the emitter of Q_{11}. Resistor R_{39} and capacitor C_{21} serve as a filter to attenuate frequencies above 20 KHz from both the input signal and the fed back signal. This network also provides phase-lag for stability of the feedback loop.

The output of the integrator, point C, and the output of the second audio amplifier, point E, are fed into the summing amplifier. This is an operational-amplifier type summing circuit. The amplifier consists of Q_{12} and Q_{13}, and is designed similarly to the first and second audio amplifiers, except for the bypassed emitter resistor of Q_{13} and a different biasing circuit. Diodes D_8 and D_9 compensate for changes in V_{BE} of Q_{12} and Q_{13} due to temperature, and rheostat R_{46} is used to set the quiescent level of the output, point F. The triangle-wave input resistor is R_{40} and the audio signal input resistor is R_{41}. Resistors R_{42} and R_{43} in parallel form the feedback resistor. Capacitor C_{22} is a high frequency bypass to insure sharp peaks on the output triangle-wave. The peak-to-peak audio amplitude at point F is "A" of Fig. 2.2.1, and the peak-to-peak sampling wave amplitude is "B" of Fig. 2.2.1.

The output of the summing amplifier feeds into the bi-level slicer, which consists of Q_{14} and Q_{15} and associated circuitry. Speed-up capacitors C_{26} and C_{27} improve the switching speed of Q_{14} and Q_{15}. Diodes D_{10} through D_{13}, bypassed by C_{25}, approximately cancel the voltage drops

across the Q_{14} and Q_{15}, providing temperature compensation. Thus, the difference between clipping levels 1 and 2 ("C" in Fig. 2.2.1) is approximately equal to the voltage drop across Zener diode D_{15} in the New Mode, or resistor R_{59} in the conventional mode. Diodes D_{14} and D_{16} prevent reverse base-emitter breakdown of Q_{14} and Q_{15}. Steady-state current through D_{15} or R_{59} is supplied by R_{53} and R_{54}. Capacitors C_{30} and C_{31} bypass both ends of D_{15} (or R_{59}) to ground at audio frequencies, while C_{32} bypasses them to each other at sampling frequencies. In the conventional mode, R_{59} provides a small voltage drop to compensate for the fact that diodes D_{10} through D_{13} have a higher steady-state current through them than the diodes whose drops they cancel, and therefore have a slightly higher drop, and the fact that the turn-on time of the transistors Q_{14} through Q_{19} is less than their turn-off time. The dc level from the "middle" of D_{15} (or R_{59}) to ground is determined partially by R_{53} and R_{54} and partially by feedback action through R_{60} and R_{61}, which will be explained later. The outputs from the bi-level slicer are taken from the collectors of Q_{14} and Q_{15}. Capacitors C_{28} and C_{29} are speedup capacitors, and R_{55} and R_{58} speed turn-off of Q_{16} and Q_{17}.

The outputs of the slicer, points G and H (the signals appearing here will be opposite in phase from those shown at points G and H in Fig. 3.1.1) are fed into the power switching transistors, Q_{16} through Q_{19}. Transistors Q_{16} and Q_{18} are connected in one type of Darlington configuration, and Q_{17} and Q_{19} are connected in another type. Thus, both transistor pairs behave essentially as single transistors with very high h_{FE}. Resistors R_{62} and R_{63} speed turn-off of Q_{18} and Q_{19}. The outputs

of the two Darlington circuits are connected together at point I which is the output, before filtering, of the amplifier.

The output filter consists of L_1 and C_{33} - a simple low-pass configuration with a cutoff frequency of 20 KHz. The small one-turn secondaries on L_1 are connected in series with R_{62} and R_{63} to provide a small amount of regeneration to speed turn-on and turn-off of relatively slow Q_{18} and Q_{19} (f_T= 10 MHz). Capacitor C_{34} prevents the 20 volts of dc appearing at point I from reaching the load.

The dc voltage at the output of the filter is fed back through R_{60} and R_{61} to insure that the waveform before the filter (point I) is symmetrical. This occurs when the average of the two slicer control values is equal to two diode drops above the dc voltage at point F. Since the supply voltage for the amplifier is 40 volts, the proper dc voltage at point I is 20 volts. This voltage is fed back to D_{15} (or R_{59}), thereby making the average of the two clipping levels also equal to 20 volts. The dc voltage at point F is set to 18.8 volts with R_{46}. Should the dc voltage at point I be lower (greater) than 20 volts, the feedback action will lower (raise) both control values, thereby increasing (decreasing) the upper pulse width and decreasing (increasing) lower pulse width. This action restores the proper voltage at point I.

The conventional mode inherently has about 5.5db more gain then the new mode. Therefore it is necessary to attenuate the feedback signal 5.5db when operating in the conventional mode, if equal feedback gain reduction is to be obtained in both modes. One section of the MODE SWITCH, together with R_{64}, R_{66} and R_{67}, is connected to accomplish this, while presenting a constant resistance of 3.9K to the feedback filter.

The feedback filter consists of R_{68}, R_{69}, C_{36} through C_{40}, and L_2 through L_4. This filter is basically a one pole RC filter (C_{36} and the 3.9K source resistance) whose capacitive element is shunted by a phase-lead network (C_{37}, R_{68}) and three series resonant elements tuned to the oscillator's fundamental, second-harmonic and third-harmonic frequencies. The 680 ohm resistor (R_{69}) lowers the "Q" of undesirable resonances. Transistor Q_{20} is an emitter follower which presents a high impedance to the filter and a low impedance to the variable attenuator following it. A voltage divider consisting of the 3.9K source impedance and the parallel combination of R_{70} and R_{71} reduces the signal input to Q_{20} slightly to keep it in its linear region. The variable attenuator consists of the voltage divider made up of R_{36} and either R_{72}, R_{73} or infinity, depending on the position of the feedback switch.

Transistor Q_7 is an emitter-follower type voltage regulator which maintains a constant fifteen volts to the oscillator, slicer and integrator circuits.

3.3 Filtering Problems

The output filter (L_1, C_{33}) acts as an integrator to the high frequency switching signal present at its input. The input to this filter has been assumed to be the theoretical output of the New Mode, i.e., that of the third waveform of Fig. 2.2.1. If the filter is removed and the waveform at point I is fed to an 8 ohm resistive load through C_{34}, the output will closely resemble the theoretical waveform. However, with the filter in, point I sees an inductive rather than a resistive load. This has a profound effect on the waveform at I.

A conventional Class D amplifier does not have any serious problem operating into an inductive load, since there is never a significant length of time when both transistors are off. In the New Mode, there is much time when neither transistor (Q_{18} or Q_{19}) is conducting. During this time, the instantaneous voltage at point I is not necessarily equal to +20 volts (zero volts with respect to the average voltage at I) as was assumed in Chapter 2 and in the block diagram (Fig. 3.1.1). For instance, when Q_{18} turns off, instead of the voltage at point I becoming +20 volts, it becomes zero volts while the current in L_1 decays to zero through D_{18}. Then the voltage at I returns to a value such that there is no voltage across L_1. Well, this is what would happen if it were not for the ringing produced in L_1 by stray capacitance of the circuit and the switching times of D_{17} and D_{18}. Neglecting these effects, we will analyze the combination of output circuit and filter.

Let us assume that the amplifier will respond to direct current, and determine the static transfer characteristic of the output and filter circuits. We will assume "ideal" New Mode with $k_d = 0$; i.e., with no modulation present the pulse width of both the upper and lower pulse trains is zero. This gives a linear overall transfer characteristic in the theoretical system of section 2.2, as indicated by the lack of harmonics of the modulating frequency in Eq. (2.2.42). We will determine the variation in dc output voltage with upper pulse train duty cycle K. The total transfer characteristic then would consist of two curves: the one we are about to derive and one obtained by rotating this curve π radians about the origin.

Figure 3.3.1 shows an equivalent circuit of the output stage and filter for positive pulses only. All components are assumed to be ideal. Switch S represents Q_{18}, which cycles open and closed at a rate F. The length of time for one on-off cycle is $T = \frac{1}{F}$, and the duty cycle of S is K. That is, the length of time S is closed during each cycle is TK, where $0 \leq K \leq 1$. We will assume that C is large enough that its voltage remains constant over the switching period, treating V_J as dc voltage. Let S close at $t = 0$. Let us assume that C has a charge of V_J volts. From $t = 0$ until $t = TK$, the voltage across L will be $V - V_J$. During this time the current through L will build up according to

$$I_L(t) = \frac{1}{L} \int_0^t (V-V_J)\, dt = t\,\frac{(V-V_J)}{L};\ 0 \leq t \leq TK \qquad (3.3.1)$$

provided that

$$I_L(0) = 0. \qquad (3.3.2)$$

This is true for small values of K, as will be apparent shortly. From Eq. (3.3.1), we get

$$I_L(TK) = \frac{TK(V-V_J)}{L} \qquad (3.3.3)$$

When S opens at TK, current through L does not change instantaneously, but continues to flow through D_1 (which represents D_{18} in Fig. 3.2.1). At this time, the voltage across L is $-(V+V_J)$, and the current through L decays according to

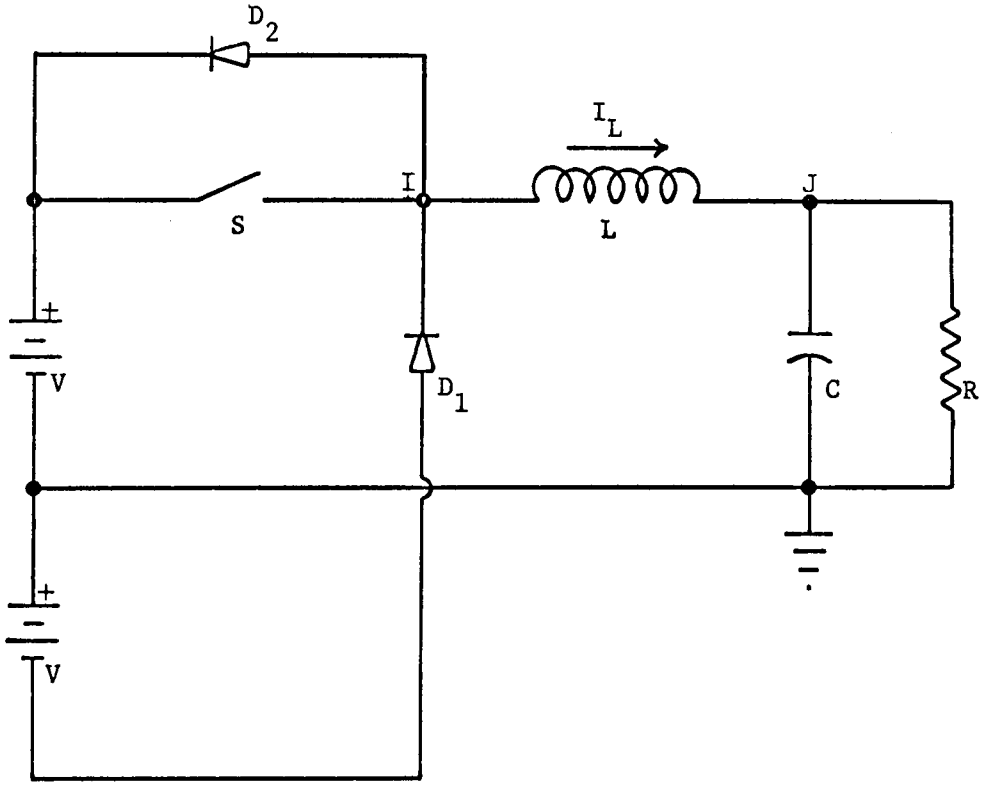

Figure 3.3.1 Equivalent circuit of amplifier output stage.

$$I_L(t) = I_L(TK) - \frac{1}{L}\int_{TK}^{t} (V+V_J)dt; \quad TK \le t \le t_1 \qquad (3.3.4)$$

$$= \frac{2TKV}{L} - \frac{tV}{L} - \frac{tV_J}{L}$$

where t_1 is the time when I_L reaches zero and D_1 stops conducting. For larger pulse widths (K > approximately 0.6) S closes again before t_1 is reached; i.e., $t_1 > T$, and current flow through L_1 is uninterrupted.

We will first consider the case of $t_1 > T$. Under this condition, when t_1 is reached, the current through the inductor is zero and remains zero until S closes again. Thus, as stated earlier, the current at the beginning of each cycle is zero.

$$I_L(t) = 0 \qquad t_1 \le t \le T \qquad (3.3.5)$$

Solving Eqs. (3.3.4) and (3.3.5) simultaneously at $t=t_1$, we get

$$t_1 = 2TK\left(\frac{V}{V+V_J}\right) \qquad (3.3.6)$$

Now, we take the average of $I_L(t)$ over one cycle:

$$I_L(\text{average}) = \frac{1}{T}\int_o^t I_L(t)dt = \frac{1}{L}\left(2Kt_1V - TK^2V - \frac{t_1^2V}{2T} - \frac{t_1^2V_J}{2T}\right) \qquad (3.3.7)$$

Substituting Eq. (3.3.6) for t_1 in Eq. (3.3.7), we get

$$I_L(\text{average}) = \frac{TK^2V}{L}\left(\frac{V-V_J}{V+V_J}\right) \qquad (3.3.8)$$

After many cycles, C will take a charge such that the average current through it is zero. Thus,

$$I_L(\text{average}) = I_R = \frac{V_J}{R} \tag{3.3.9}$$

Substituting Eq. (3.3.8) into Eq. (3.3.9), and solving for V_J, we obtain

$$V_J = \frac{V}{2}\left[-1 - AK^2 + (1+5AK^2+A^2K^4)^{\frac{1}{2}}\right] \tag{3.3.10}$$

where

$$A = \frac{TR}{L} \tag{3.3.11}$$

Substituting Eq. (3.3.10) into Eq. (3.3.6) for V_J, we obtain

$$t_1 = \frac{4TK}{1-AK^2+(1+5AK^2+A^2K^4)^{\frac{1}{2}}} \tag{3.3.12}$$

There is a value of K for which $t_1=T$. Substituting T for t_1 in Eq. (3.3.12) and solving for K, we get

$$K = \frac{-2+\frac{7}{8}A+\left(4+\frac{1}{2}A+\frac{49}{64}A^2\right)^{\frac{1}{2}}}{2A} \tag{3.3.13}$$

At this value of K, we can solve for V_J by substituting $t_1=T$ into Eq. (3.3.6)

$$V_J = V(2K-1) \;;\; t_1 = T \tag{3.3.14}$$

If $t_1>T$, then current flows through L at all times. Since the voltage waveform at node I is simply defined for $t_1 > T$ by

$$V_I(t) = V \; ; \; 0 < t < TK$$

$$V_I(t) = -V \; ; \; TK < t < T \tag{3.3.15}$$

Since the average (dc) voltage across an ideal inductor must be zero,

$$V_J = V_I(\text{average}) = \frac{1}{T}\int_o^t V_I(t)dt = V(2K-1); \; t_1 > T \tag{3.3.16}$$

Note that this is the same as Eq. (3.3.14).

Substituting the following quantities:

$$T = 1/F = 10^{-5} \tag{3.3.17}$$

$$R = 8, \tag{3.3.18}$$

$$V = 20, \tag{3.3.19}$$

and

$$L = 62 \times 10^{-6} \tag{3.3.20}$$

into Eqs. (3.3.11) and (3.3.10), we obtain

$$V_J = -10 - 12.9K^2 + 10\,(1 + 6.45K^2 + 1.664K^4)^{1/2}; \; 0 \le t_1 \le T \tag{3.3.21}$$

The value of K for which $t_1 = T$ is, from Eq. (3.3.13)

$$K = 0.6054 \; ; \; t_1 = T \tag{3.3.22}$$

For values of K larger than the above, the curve of K vs. dc output voltage follows Eq. (3.3.16):

$$V_J = 40K - 20 \; ; \; t_1 \ge T \tag{3.3.23}$$

A computer program was written to compute values of dc output voltage (V_J) for values of K from 0 to 1, in increments of 0.01,

following Eq. (3.3.21) for K=0.00 to K=0.60, and following Eq. (3.3.23) for K=0.61 to K=1.00. These values were plotted vs. K on a CalComp Pen Plotter, and this plot is shown in Fig. 3.3.2. The small "+" mark on the graph is at K=0.61, the lowest value of K for which Eq. (3.3.23) was used. The CalComp Plotter connected each of the 101 computed points with straight line segments to produce this plot. (See Appendix B for program and calculated values.) The ideal shape for this curve would obviously be a straight line connecting the end points. This is the shape the curve would have if the voltage waveform at the filter input were that of the "ideal" New Mode described in section 2.2. The curve of Fig. 3.3.2 is far from ideal, however!

The portion of the curve to the left of the "+" mark is fairly linear except near the origin. This curve asymptotically approaches zero output as K approaches zero. This means that substantially no output will result for very small values of K.

The curve of Fig. 3.3.2 represents only one half of the amplifier transfer characteristic, however. The actual characteristic consists of two such curves as shown in Fig. 3.3.3. Figure 3.3.3.(a) shows the composite characteristic for the case of no pulse overlap; i.e., $k_d=0$. Setting k_d equal to a small positive value effectively shifts the upper curve to the left and the lower curve to the right as shown in Fig. 3.3.3(b). Actually, for the portion of the curve between the K origin and K′ origin, the presence of the lower-train pulses modifies slightly the shape of the upper curve, and vice versa. This is apparent, since t_1 is a function of output voltage V_J (Eq. (3.3.6)). However, this slight effect can be neglected, since V_J is small in the region of concern anyway. The

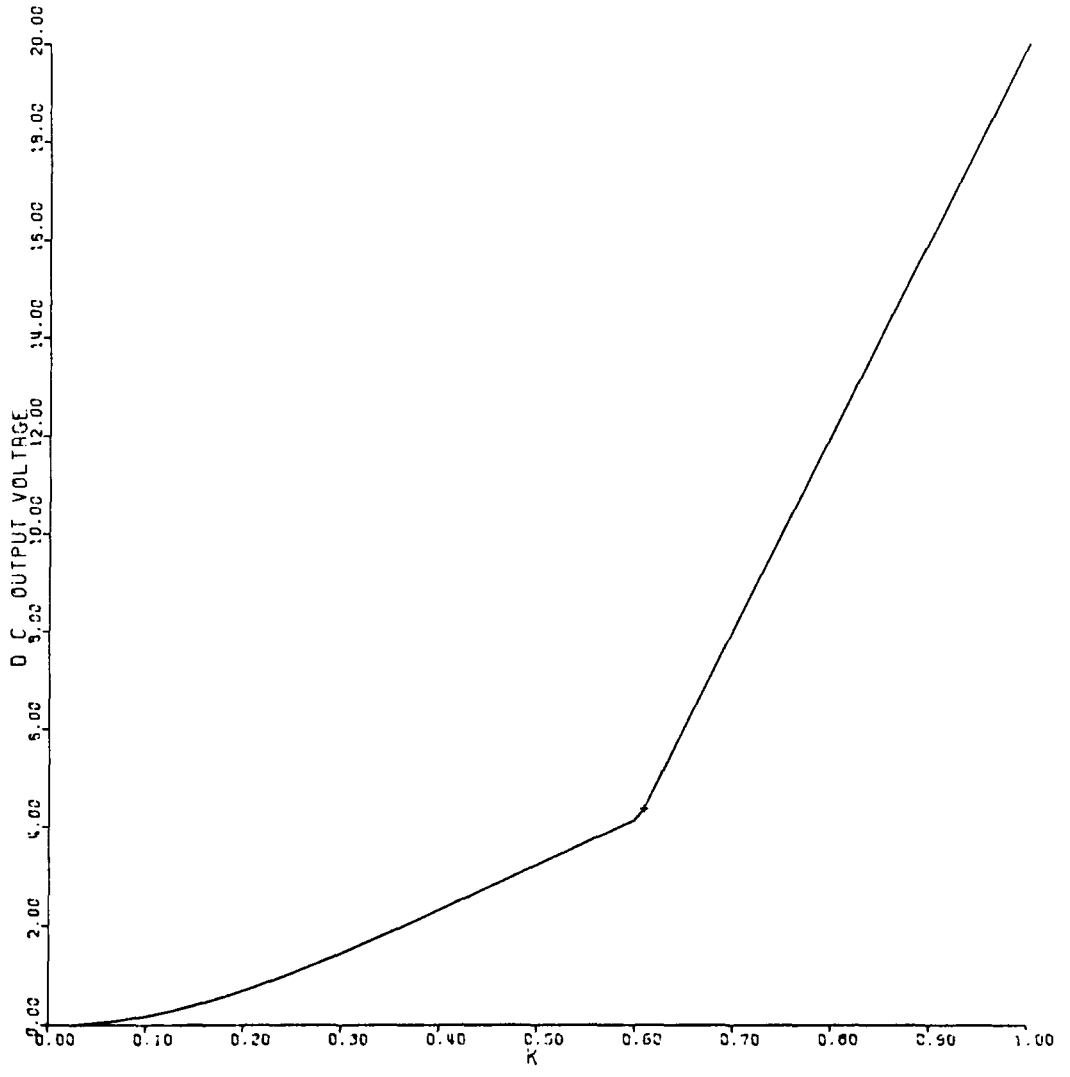

Fig. 3.3.2. Computer-plotted transfer characteristic of circuit Fig. 3.3.1.

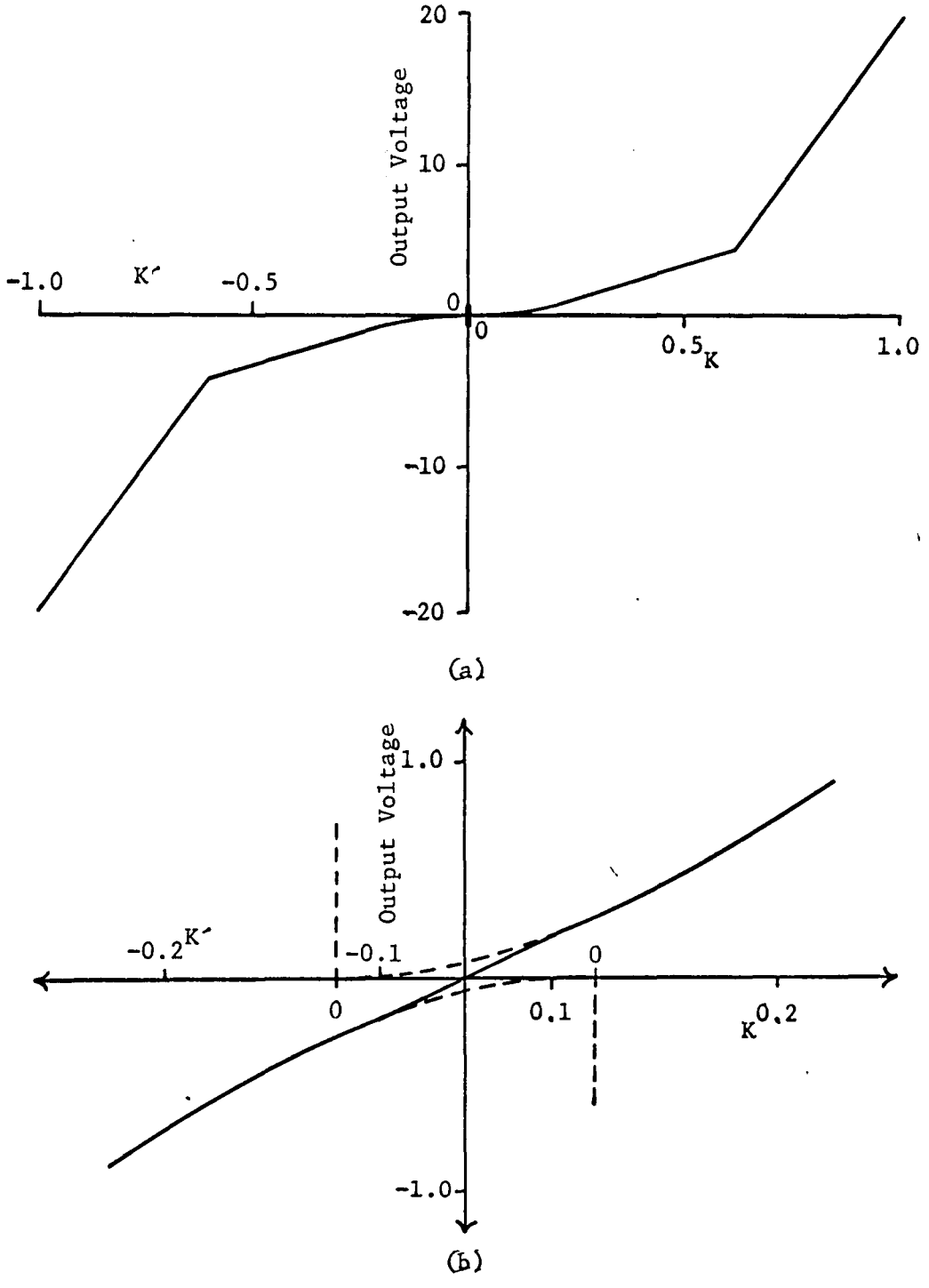

Fig. 3.3.3. Composite transfer characteristics of complete output circuit. (a) Characteristics with k_d=0; (b) Center portion of characteristics with k_d=0.12.

composite curve shows significantly reduced nonlinearity near the origin.

Since the ideal characteristic, considering the upper right-hand quadrant only, is a straight line connecting the origin and the end point (K=1, V=20) it seems that it would be desirable to rotate the left portion of the curve (Eq. (3.3.10)) counterclockwise so that it would intersect the end point.

Setting K equal to unity in Eq. (3.3.10), we find that V_J approaches V only as A approaches infinity, if we limit ourselves to positive values of A. Large A implies small L, keeping load resistance and switching frequency constant. The smaller L becomes, the larger C must become to retain proper filtering action, and the larger the switching currents through the output transistors become, lowering efficiency. A value of 62 μH was chosen for L as a compromise between efficiency, linearity, and C required for proper filtering.

Figure 3.3.4 shows the output of the amplifier with a 1000 Hz sine wave input, using the New Mode, without feedback and with R_{65} removed. The presence of the 100 KHz switching frequency, due to imperfect filtering, is clear in the photograph. Note that the nonlinearity near the dc axis has been reduced by setting k_d=0.1 instead of zero.

Four "plateaus" occur during each cycle of the input signal, two of which occur at A and B, Fig. 3.3.4. These occur at points on the transfer characteristic which correspond to the "+" mark on Fig. 3.3.2. The equations derived earlier do not predict these regions where an increase in pulse width does not produce a corresponding increase in output. This effect is produced by ringing (damped oscillation) of L. While stray capacitance (of transistors, diodes and inductor) contributes somewhat

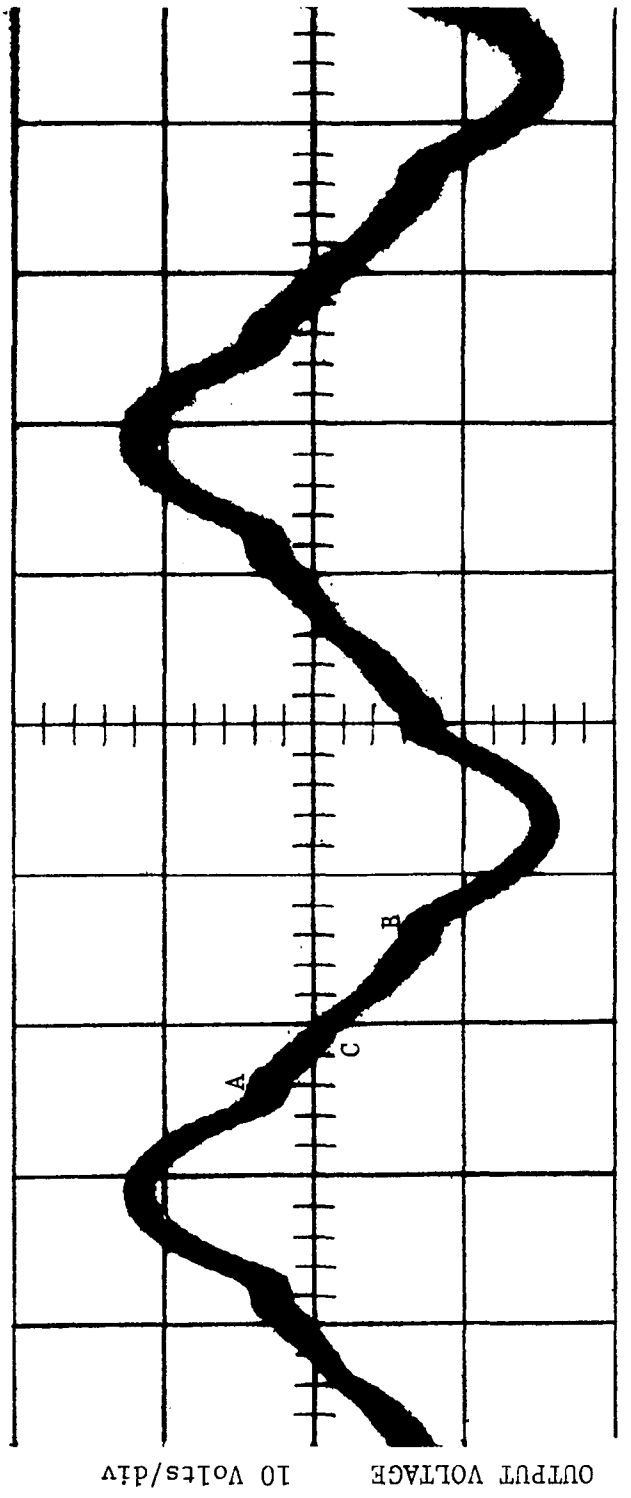

Fig. 3.3.4. Output of amplifier in New Mode with 1000 Hz input with R_{65} removed and without feedback.

to this ringing effect, the principal cause is the storage time of diodes D_{17} and D_{18}. Referring to Fig. 3.3.1, this storage time produces ringing in the following manner: When the current in L decays to zero at time t_1 ($t_1 < T$ for ringing to occur), D_1 does not stop conducting immediately, but continues to conduct until a small current in the reverse direction has built up in L. When D_1 finally stops conducting at t_1', (see Fig. 3.3.5 (a)) this reverse current in L causes the voltage at node I to rise until D_2 begins to conduct. The same phenomenon occurs with D_2, and the ringing continues. The ringing is sufficiently damped so that the diodes contribute to the ringing for only one oscillation, as in Fig. 3.3.5 (a). After t_2', the ringing is due entirely to stray capacitance.

The effect this ringing has on circuit performance is as follows: As long as $t_2' < T$, there is a negligible effect, since the additional time D_1 conducts, from t_1 to t_1', is largely offset by the conduction of D_2. When pulse width (time S is closed) increases to the point where t_2' is greater than T, but t_1' is still less than T, the beginning of the next pulse is lost, as shown in Fig. 3.3.5 (b). As K is increased from the point where $t_2' = T$ to the point where $t_1' = T$, no change in actual pulse width ($T + TK - t_1'$) occurs, and, therefore, no change in output occurs.

The presence of these regions of constant output for changing input is very bad from a distortion standpoint. The sharpness of these plateaus causes distortion which is rich in higher-order harmonics, which are generally more objectionable than lower-order ones. Also, it is harder for negative feedback to compensate for regions of zero gain

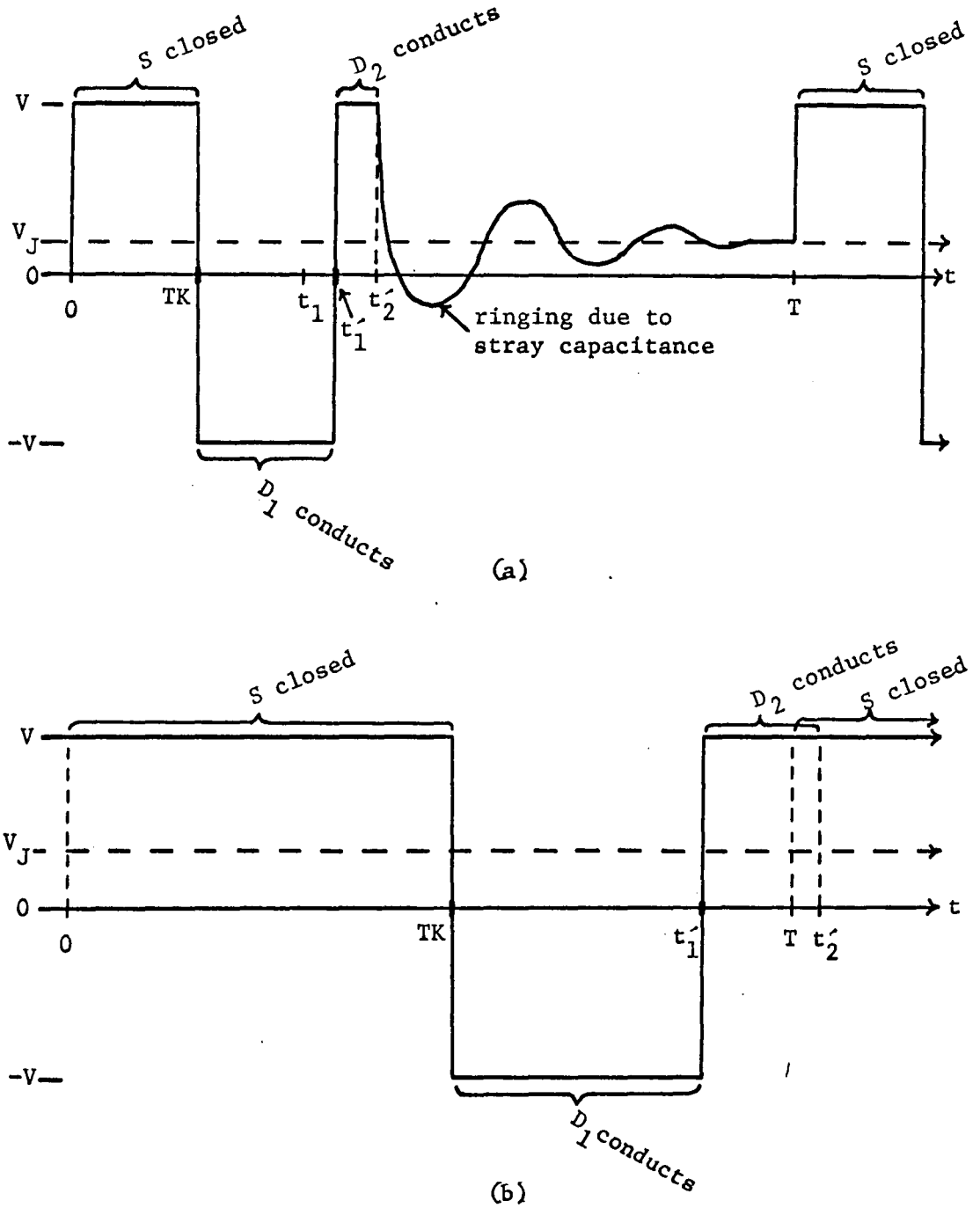

Fig. 3.3.5. Voltage waveform at Node 1 of Fig. 3.3.1.
(a) Waveform for K ≈0.2. (b) Waveform for K ≈0.6.

in the transfer characteristic. Therefore, it is advisable to try to smooth out these regions as much as practical. The original diodes used for D_{17} and D_{18} were replaced with special fast-switching types, (t_{RR}=100nsec.) using three in parallel to handle the current and to reduce forward voltage drop. This greatly reduced the width of these plateaus. The remainder of the ringing was removed by shunting L with a resistor (R_{65}). The value chosen, 235 ohms, was the largest value resistor that would prevent D_2 (Fig. 3.3.1) from conducting (i.e., $t_2' = t_1'$) for all times when $t_1' < T$. This effectively eliminated all regions of zero gain.

Figure 3.3.4 was the output of the amplifier without the damping resistor, but with the fast-switching diodes. (The earlier design with the slow-switching diodes had much worse plateaus.) Figure 3.3.6 shows the result of adding R_{65}. As this resistor serves no purpose when this amplifier is operated in the conventional mode, but does lower efficiency somewhat, it is switched out of the circuit when operating in the conventional mode.

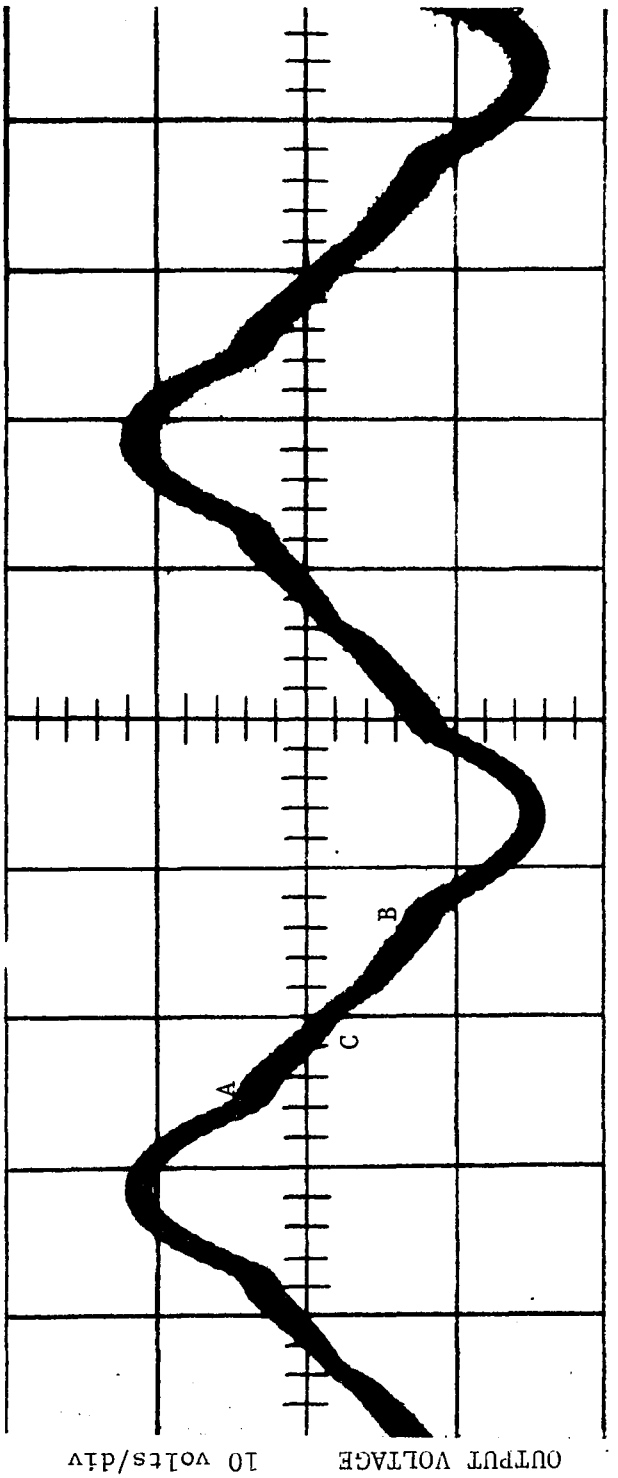

Fig. 3.3.6. Output of amplifier in New Mode with 1000 Hz input, without feedback.

CHAPTER IV

PERFORMANCE OF THE AMPLIFIER IN BOTH MODES

In this chapter, a thorough comparison of the efficiency and distortion characteristics of the two modes is made, for the three different amounts of feedback.

4.1 Efficiency Characteristics

The value of efficiency presented in this chapter are values of overall circuit efficiency. That is,

$$\eta = \frac{\text{Total dc power in}}{\text{Total power out}} \qquad (4.1.1)$$

A measure of "output stage" efficiency would have been somewhat more meaningful, but, due to the difficulty of separating the output stages from the rest of the circuit, overall efficiency was measured. The power consumed by stages other than the driver and output is only about a watt, however, so the difference between the two types of efficiency is small.

The output of the amplifier contains components at frequencies other than the input frequency. Therefore an efficiency based on desired-output power, rather than total output power, would be more useful in some instances. We therefore define the desired-output efficiency as

$$\eta_{d.o.} = \frac{\text{Total dc power in}}{\text{Desired-signal power out}} \qquad (4.1.2)$$

and the desired-output factor as

$$F_{d.o.} = \frac{\text{Desired output (voltage)}}{\text{Total output (voltage)}} \qquad (4.1.3)$$

This factor was determined by measuring the output of a 1 KHz parallel-resonant filter driven by the amplifier. The output of the amplifier, which was driven by a 1 KHz sine wave generator, was adjusted to 8 volts RMS. The filter was then driven by an 8 volt sine wave source, and its output was again measured. The ratio of these two filter output voltages is the desired-output factor.

The relationship between the two efficiencies is

$$\eta_{d.o.} = \eta F^2_{d.o.} \qquad (4.1.4)$$

All ac voltages were measured on a Ballantine 323 True-RMS voltmeter. All dc voltages were measured on a Hewlett-Packard 410 B voltmeter, and all direct currents were measured on a Triplett 630-A multimeter. The signal source was a Wavetek 114 function generator (sine-wave output used), with a three-pole R-C low-pass filter at its output to remove unwanted harmonics. An 8-ohm (±3%) seventy-watt resistor was used as an output load for all measurements, including those taken under no-signal conditions.

4.1.1 Idling Properties

Table 4.1.1 gives no-signal values of input current, input power and output voltage for both modes, for the three different amounts of feedback. The supply voltage was maintained at a constant 42 volts.

The New Mode idling current is, as one would expect, much lower than that of the conventional mode. But, when maximum feedback was applied, the quiescent current and output voltage of the New Mode increased and became comparable with those of the conventional mode.

TABLE 4.1.1

IDLING PROPERTIES OF DUAL-MODE AMPLIFIER

Mode	Feedback Position	V_{OUT} (RMS Volts)	I_{in} (mA)	P_{in} (Watts)
Conv.	3 (none)	.82	123	5.17
Conv.	2 (low)	.82	124	5.21
Conv.	1 (high)	.82	126	5.29
New	3	.12	52	2.18
New	2	.17	64	2.69
New	1	.45	118	4.96

This dependence of input power on the amount of feedback occurs under signal conditions too, where the conventional mode is most affected, as will be seen later.

Figure 4.1.1 (a) shows the quiescent waveform appearing at point F, Fig. 3.2.1 (the output of the summing amplifier) when no feedback is used. This is the pure, unmodulated sampling triangle-wave. (Note the high degree of asymmetry. This was necessary to obtain high efficiency in the conventional mode, as explained in section 3.2.) But, when feedback is added, this waveform becomes distorted. This effect is due to an imperfect feedback filter passing some of the switching-signal harmonics, allowing them to mix with the modulating signal in the summing amplifier. The highly distorted waveform of Fig. 4.1.1 (b) (New Mode with maximum feedback), when passed through the bi-level slicer and output circuits, increases the dissipation in these latter circuits and changes the quiescent waveform at point I (Amplifier output before filtering). This distortion of the triangle-wave is worse in the New Mode, since more signal is fed back to compensate for its inherent lower gain, as explained in section 3.2. However, due to the longer time between positive and negative output pulses in the New Mode, the effect of this triangle-wave distortion on output circuit dissipation is far less serious.

Figure 4.1.2 (a) shows the output of the amplifier in the New Mode without feedback, with the output filter removed. That is, L_1 is shorted and C_{33} is opened. (Note the poor rise and fall times of the pulses due to the slowness of the power transistors.) From calculations based on this photograph, the no-signal power dissipated in the load is

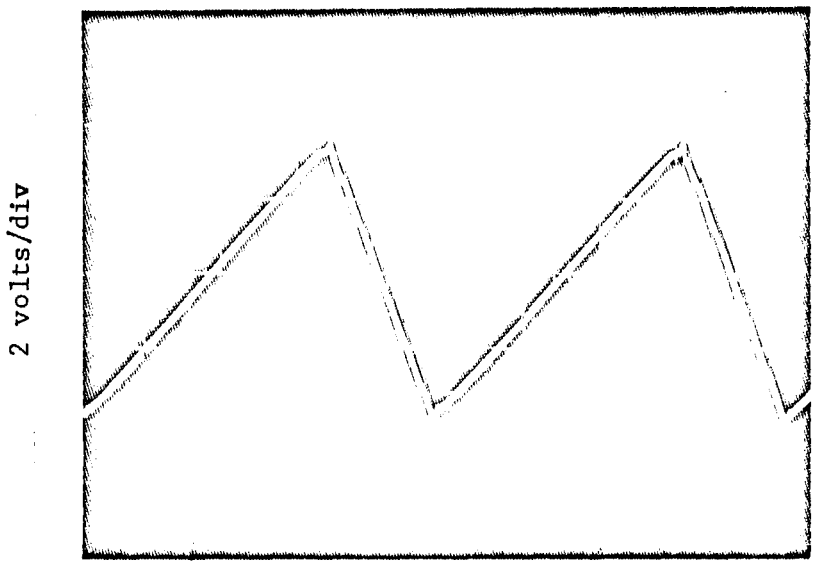

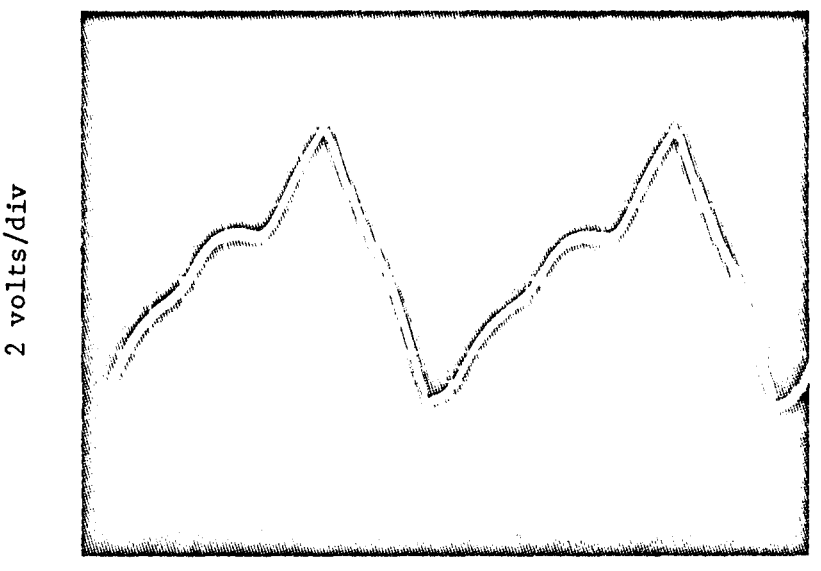

Fig. 4.1.1. Quiescent voltage waveform at point F, Fig. 3.2.1. (a) New Mode without feedback. (b) New Mode with high feedback.

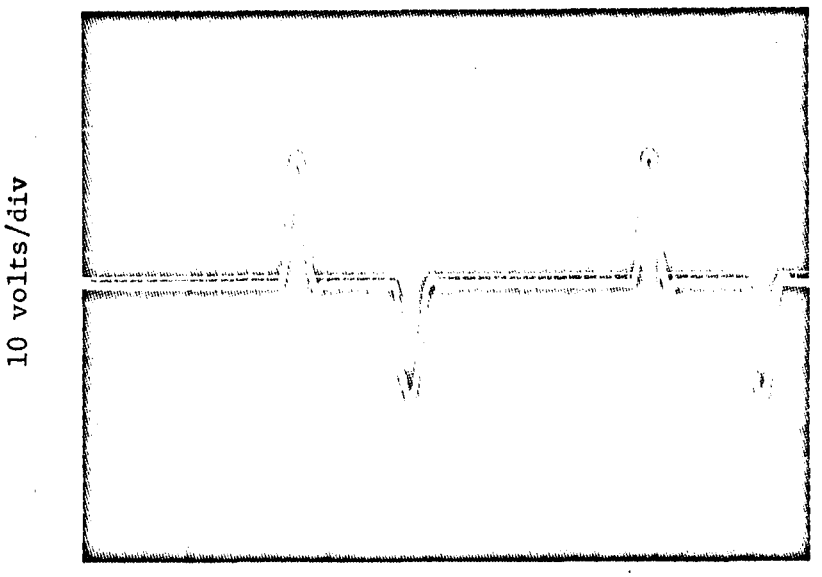

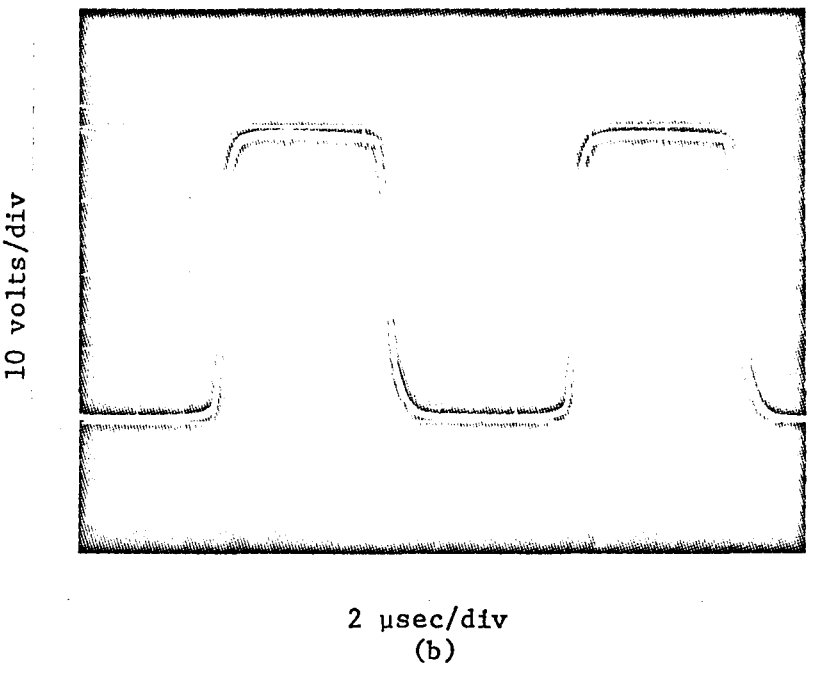

Fig. 4.1.2. No-signal output waveform with filter removed without feedback. (a) New Mode; (b) Conventional mode.

approximately 2.3 watts. This compares with approximately 40 watts of dissipation, similarly calculated from Fig. 4.1.2 (b), which is the no-signal output in the conventional mode without feedback or filtering! When no filtering is used at the output of a switching mode amplifier, the New Mode is analogous to Class D operation, while the conventional mode is analogous to Class A operation. The difference is that in normal Class A or B, the dissipation takes place in output transistors, while in the unfiltered switching mode, this dissipating takes place in the load itself.

Figure 4.1.3 is the no-signal waveform at point 1 (New Mode, no feedback) with the output filter re-inserted. Note the greater pulse amplitude due to reduced high-frequency loading, and the highly damped (by R_{65}) ringing.

4.1.2 Low Frequency Efficiency

Table 4.1.2 gives values of efficiency and desired-output-efficiency for all combinations of mode and feedback, at 1 KHz. Output power was eight watts total (eight volts true RMS across eight-ohm load) and input voltage was 42.0 volts.

As in the no-signal case, input power increased with increasing feedback. However, with signal present, the effect was much more pronounced in the conventional mode. This phenomenon is due to the very short time, in the conventional mode, between the switching off of one output transistor and the switching on of the other, which becomes shorter because of the distortion of the sampling trianglewave.

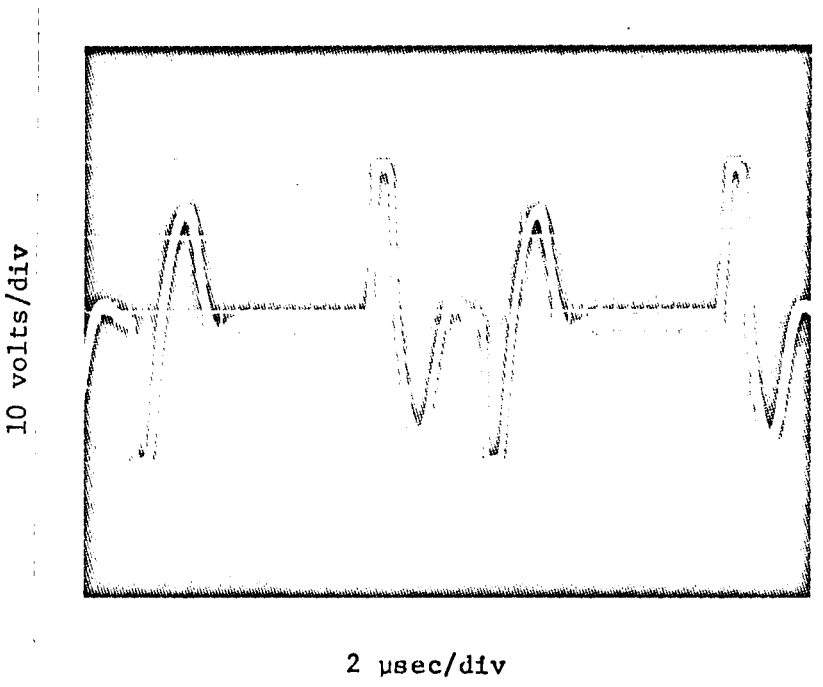

Fig. 4.1.3. No-signal waveform at point I (before filter) in New Mode without feedback.

TABLE 4.1.2

EFFICIENCIES OF DUAL-MODE AMPLIFIER

AT 1 KHz AND 8 WATTS OUTPUT

Mode	Feedback Position	I_{in} (mA)	P_{in} (Watts)	η (%)	$F_{d.o.}$	$\eta_{d.o.}$ (%)
Conv.	3	365	15.3	52.3	.986	50.8
Conv.	2	370	15.5	51.6	.986	50.1
Conv.	1	450	18.9	42.3	.986	41.1
New	3	345	14.5	55.2	.972	52.2
New	2	355	14.9	53.7	.986	52.2
New	1	365	15.3	52.3	.986	50.8

The values of $F_{d.o.}$ were fairly independent of mode and feedback (except for the highly distorted New Mode output without feedback). This indicates that most of the undesired output occurs at frequencies outside the passband of the feedback filter. This undesired output is primarily the 100 KHz switching signal leaking through the output filter. Since the values of $F_{d.o.}$ were very close to unity, and extremely close to each other, there is little value in calculating both total-output efficiency and desired-output efficiency. Therefore only total-output efficiency, η was calculated for the remaining measurements.

Efficiency data was taken at 100 Hz under conditions comparable to those for the 1 KHz measurements. In every case, the efficiency at 100 Hz was within 1 1/4% of the corresponding efficiency at 1 KHz.

4.1.3 High Frequency Efficiency

Table 4.1.3 gives efficiency data for the dual-mode amplifier at 10 KHz. Power output was 8 watts total, and input voltage was 42.0 volts, as in the previous cases.

This data indicated the clear superiority in efficiency of the New Mode at high frequencies, particularly if a large amount of feedback is used. With a modulating signal of 10 KHz, there is much energy (in the unfiltered output) at frequencies of 80 KHz, 90 KHz, 110 KHz, 210 KHz, etc., which are not efficiently filtered out by the type of feedback filter used. These unfiltered sum-and-difference frequencies cause severe distortion of the sampling triangle-wave, and increase dissipation. The New Mode is more tolerant of sampling-wave distortion, and, therefore, its efficiency remains high in spite of it. Also, high

TABLE 4.1.3

EFFICIENCIES OF THE DUAL-MODE AMPLIFIER

AT 10 KHz AND 8 WATTS OUTPUT

Mode	Feedback Position	I_{in} (mA)	P_{in} (watts)	η (%)
Conv.	3	400	16.8	47.6
Conv.	2	420	17.6	45.5
Conv.	1	550*	23.1	34.6
New	3	365	15.3	52.0
New	2	367	15.4	52.0
New	1	382	16.0	50.0

*Current was increasing rapidly under these conditions, indicating presence of thermal runaway.

frequency operation affects the conventional mode's critical balance between the switching times of both halves of the output circuit, thereby increasing dissipation, even when no feedback is used. Since the New Mode does not require this critical balance, it is less affected by high frequency operation.

4.2 Distortion Characteristics

Distortion was measured using a home-made notch-filter system consisting of a twin-tee notch filter and two operational amplifiers.

A simplified schematic is shown in Fig. 4.2.1. The twin-tee capacitors are switchable to cover a wide range of frequencies (140 Hz to 70 KHz), and two of the twin-tee resistors have both a coarse and a fine adjustment for very precise nulling. The feedback arrangement used reduces the attentuation of the second harmonic of the filter notch frequency to about 1 db. Higher harmonics of the filter frequency are negligibly affected. This is approximately a three-to-one improvement over the use of a twin-tee alone.

The equipment set-up for measuring distortion is shown in Fig. 4.2.2. A low-pass filter at the signal generator output removes most of its distortion. This filtered sine wave is fed into the amplifier, and its output is adjusted to 8 volts by means of the volume control.

Since we are only concerned about distortion within the audible range, a properly-terminated 6-pole Butterworth low pass filter is used to remove all output signals above 20 KHz. With the twin-tee filter switched out, the notch-filtering system's input level control is adjusted to obtain a one-volt reading on the true-RMS voltmeter. When

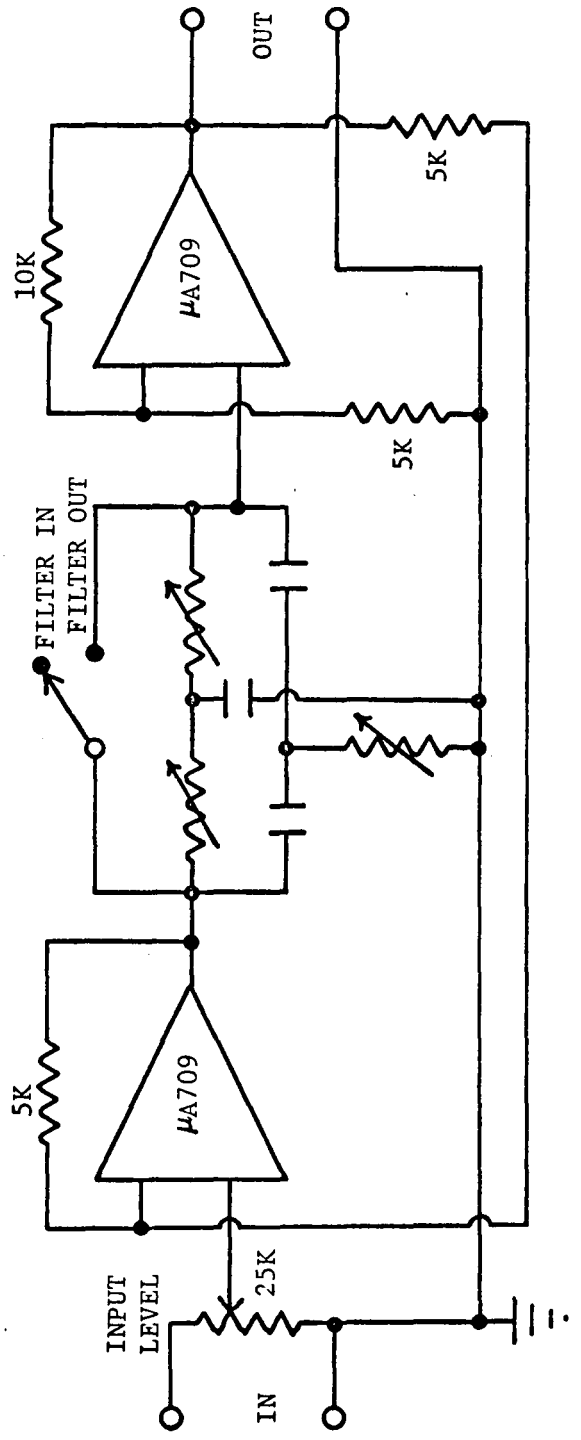

Fig. 4.2.1. Simplified schematic of distortion-measuring notch filter system.

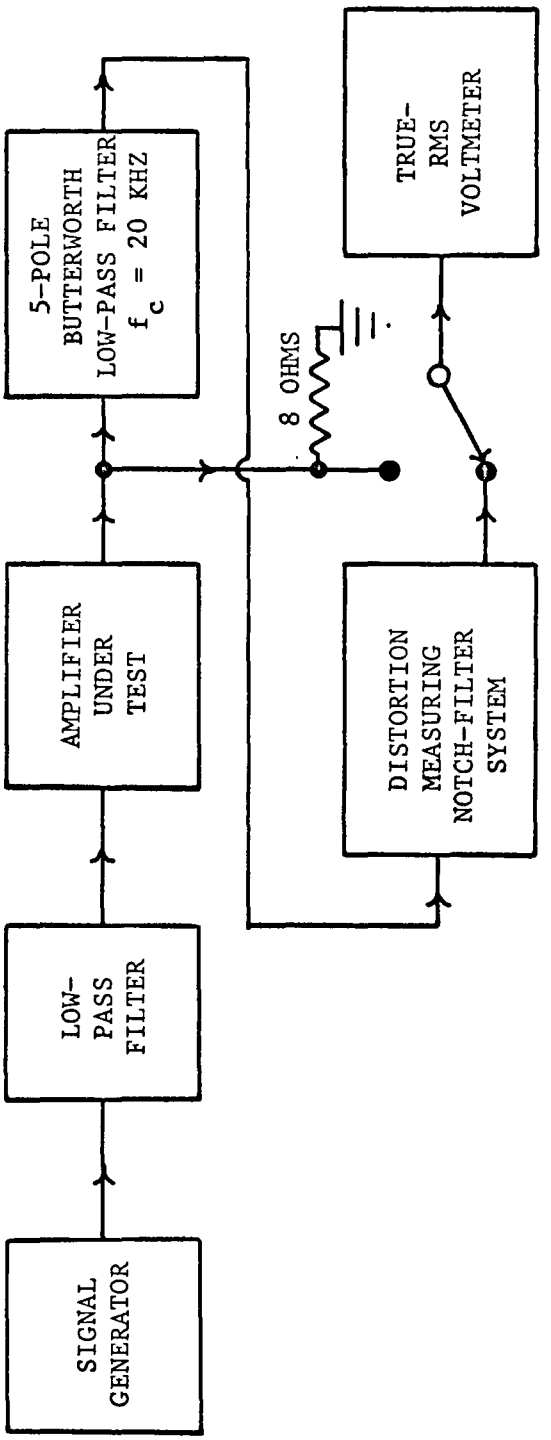

Fig. 4.2.2. Equipment set-up for measuring distortion.

the filter is switched in and tuned to null out the fundamental, the voltmeter reading in volts is equal to the distortion (e.g., 10mV = 1% total harmonic distortion). Residual system distortion (entire system less amplifier) was 0.16% at 140 Hz, 0.34% at 1 KHz, and 0.25% at 4 KHz.

4.2.1 Low Frequency Distortion

Table 4.2.1 gives distortion data for the dual-mode amplifier, with forty-two volts in and eight watts out, at 1 KHz and 140 Hz. Reciprocal relative gains and the gain reduction due to feedback in db are also given in this table to aid in evaluating the effect of the feedback. These values were measured at 1 KHz.

Both tone controls were set to their minimum position for the 1 KHz measurements, which filters out some of the distortion generated by the signal generator. This, plus the inaccuracy of measurement of very low distortion levels, may explain why the 1 KHz distortion in the conventional mode, with maximum feedback, was equal to the residual system distortion.

It is apparent from Table 4.2.1 that the New Mode has about twice as much distortion as the conventional mode. The percent distortion without feedback was approximately the same at 1 KHz and 140 Hz, but, when feedback was added, there was considerably less distortion at the lower frequency. This is due to some of the higher harmonics of 1 KHz being filtered out of the fed-back signal by the feedback filter and C_{21}.

To gain a better insight into the nature of these distortions, several photographs of output waveforms under various conditions were

TABLE 4.2.1

DISTORTIONS OF DUAL-MODE AMPLIFIER

AT 1 KHz AND 140 Hz

Mode	Feedback Position	$(\text{Rel.Gain})^{-1}$	db Feedback	% Distortion at 1 KHz	% Distortion at 140 Hz
Conv.	3	1.00*	0	8.7	8.5
Conv.	2	3.12	9.9	2.5	2.0
Conv.	1	14.6	23.3	0.34	0.45
New	3	1.96	0	18.0	18.0
New	2	5.49	8.9	5.8	4.6
New	1	24.8	22.0	1.46	1.1

* Reference.

taken. As usual, the amplifier supply voltage was 42 volts, and its output was 8 volts RMS except in Fig. 4.2.9.

Spectrum photographs of the first ten harmonics of several of the waveforms were also taken. These spectra were displayed on an old Singer SPA-3 spectrum analyzer, after allowing about two hours for it to stabilize. A logarithmic vertical scale was used on all spectra, with the uppermost division line as approximate reference level, and the bottom division line corresponding to -45 db. The spectral line closest to the extreme left-hand division line corresponds to zero frequency--its presence is strictly a property of the analyzer. (Disregard anything to the left of this line.) The fact that many of the spectral lines do not line up with the scale division lines is due to the extreme difficulty in adjusting this RF spectrum analyzer for operation at audio frequencies.

Figure 4.2.3 (a) shows the output of the amplifier in the New Mode with maximum feedback at 1 KHz. From Table 4.2.1, the distortion is 1.46%. The distortion is in the form of a sharp "kink" in the waveform, and is rich in higher harmonics, as shown in Fig. 4.2.3 (b). (Note the eighth, ninth and tenth harmonics.) This is due to the inability of the feedback to remove high frequency distortion, particularly near the crossover point. Distortion is less of a problem at lower frequencies, as Fig. 4.2.4, taken at 90 Hz, shows.

The output waveform of the conventional mode at 1 KHz with maximum feedback is shown in Fig. 4.2.5. There is no kink in the waveform, as there is no crossover. The distortion measured a very low 0.34%. (The author measured it three times just to be sure!) The high-frequency

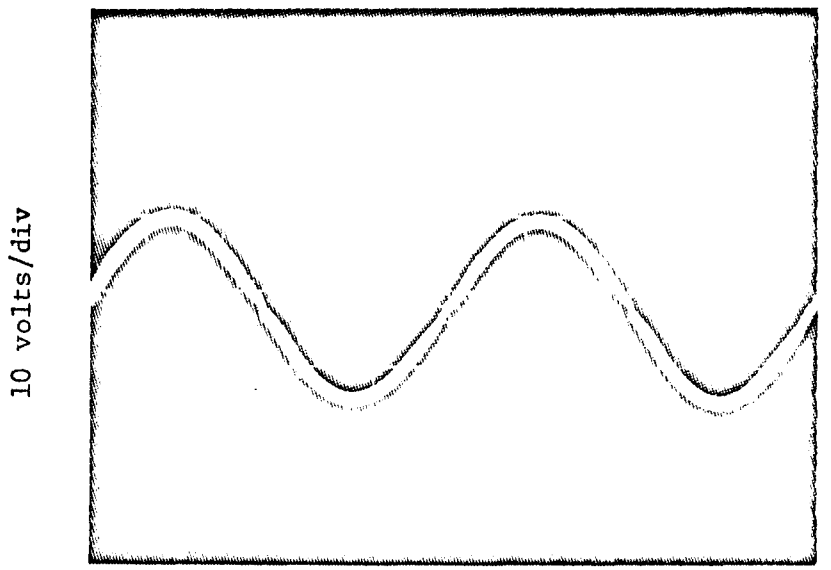

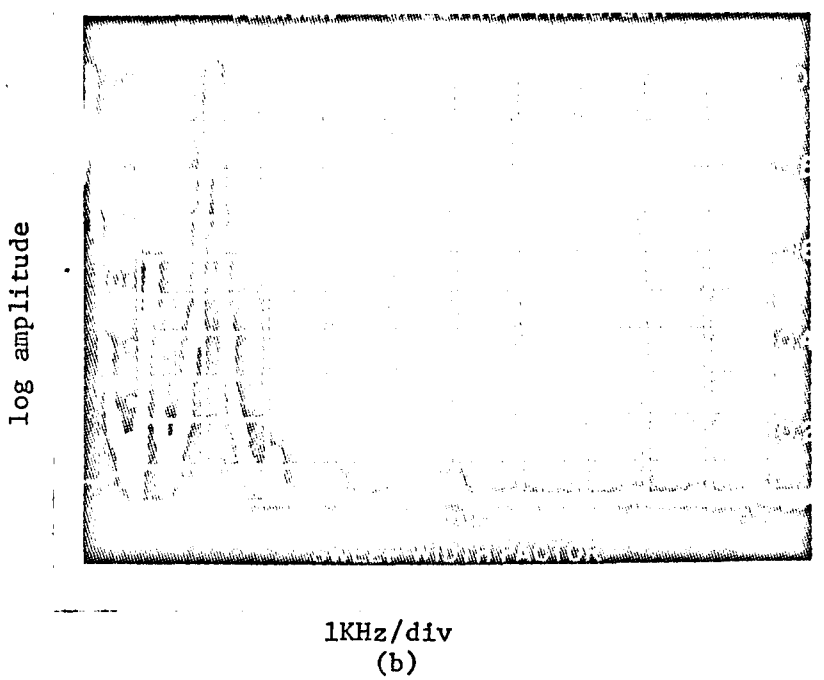

Fig. 4.2.3. Output waveform (a) and spectrum (b) of New Mode with maximum feedback at 1 KHz.

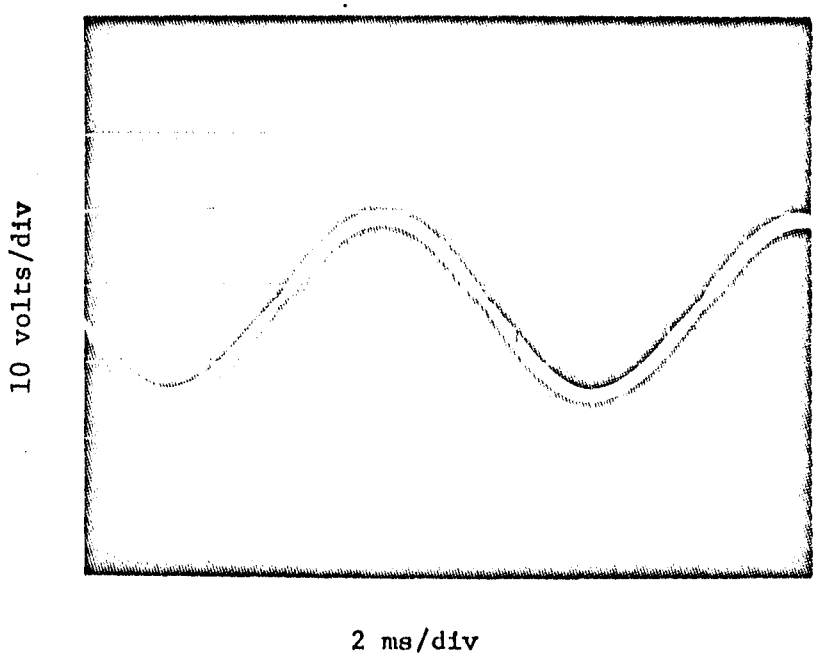

Fig. 4.2.4. Output waveform in New Mode with maximum feedback at 90 Hz.

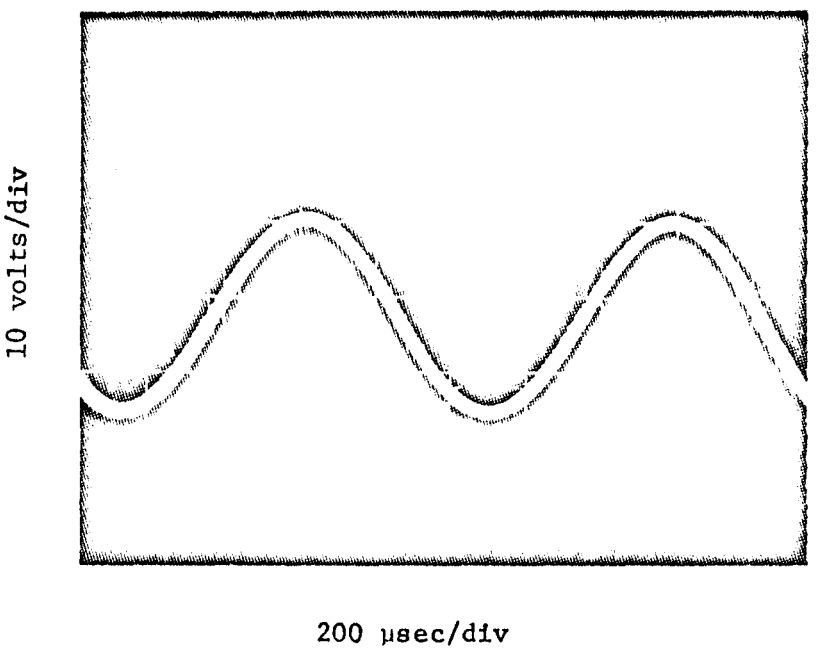

Fig. 4.2.5. Output waveform in conventional mode with maximum feedback at 1 KHz.

switching content of this waveform is somewhat greater than that of the New Mode, however.

The output waveform of the conventional mode without feedback, along with its spectrum, is shown in Fig. 4.2.6. This waveform shows much more distortion than the conventional mode is theoretically capable of. This is partly due to the fact that the amplitude of the output pulse-width-modulated waveform (before filtering) is not constant. This amplitude modulation is due to the fact that, for positive pulses, if D_{17} is conducting, the voltage at point I (Fig. 3.2.1) is 0.7 volts above B+, but if Q_{18} is conducting, this voltage is approximately a volt below B+. This same effect occurs for negative pulses with Q_{19} and D_{18}. This effect, which also affects the New Mode, has been discussed by Josephson [13], and Bach et al.[14]. The slow switching speed of the 2N1724 output transistors, which is a function of collector current and operating temperature, causes additional distortion of the output pulses.

Figure 4.2.7 shows the output of the New Mode without feedback at 1 KHz. (Figure 4.2.7 (a) is identical to Fig. 3.3.6.) Since output transistor dissipation and collector current are lower in the New Mode, the output waveform more closely approaches the theoretical. Note the symmetry of the waveform, and the lack of strong even harmonics in the spectrum. In contrast, the conventional mode exhibited a large second-harmonic (Fig. 4.2.6 (a)). However, the New Mode output contains objectionable higher harmonics which the conventional mode output does not.

The output filter was removed by shorting L_1 and opening C_{33}. The resulting waveform was integrated with a three-pole R-C filter with a

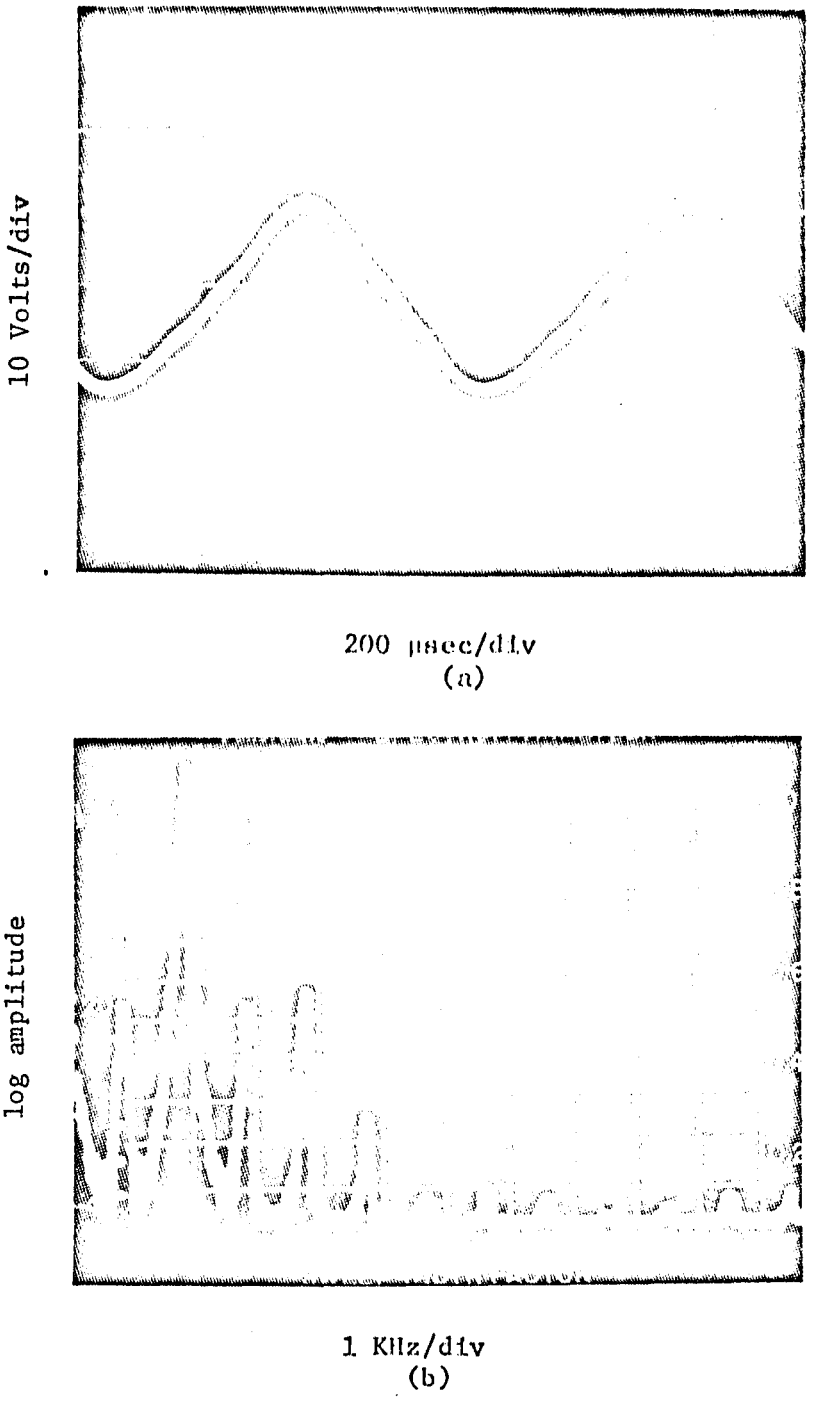

Fig. 4.2.6. Output waveform (a) and spectrum (b) of conventional mode without feedback at 1 KHz.

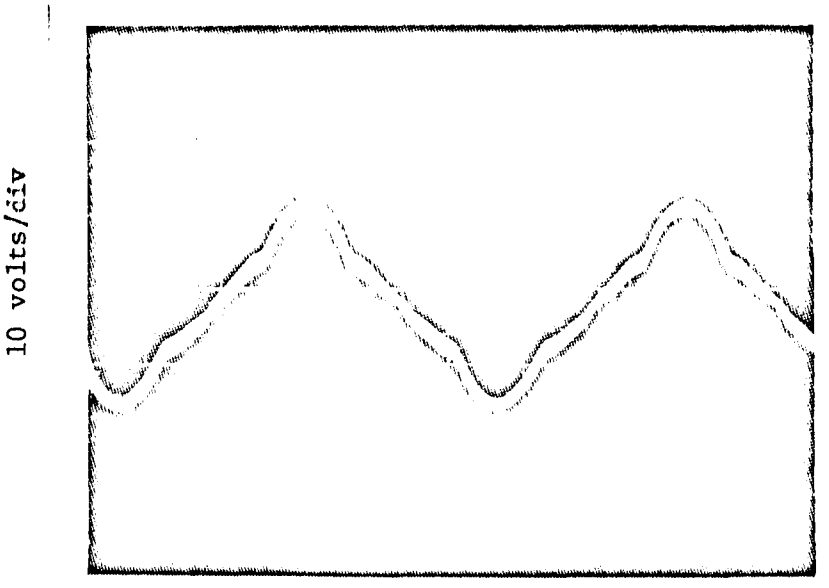

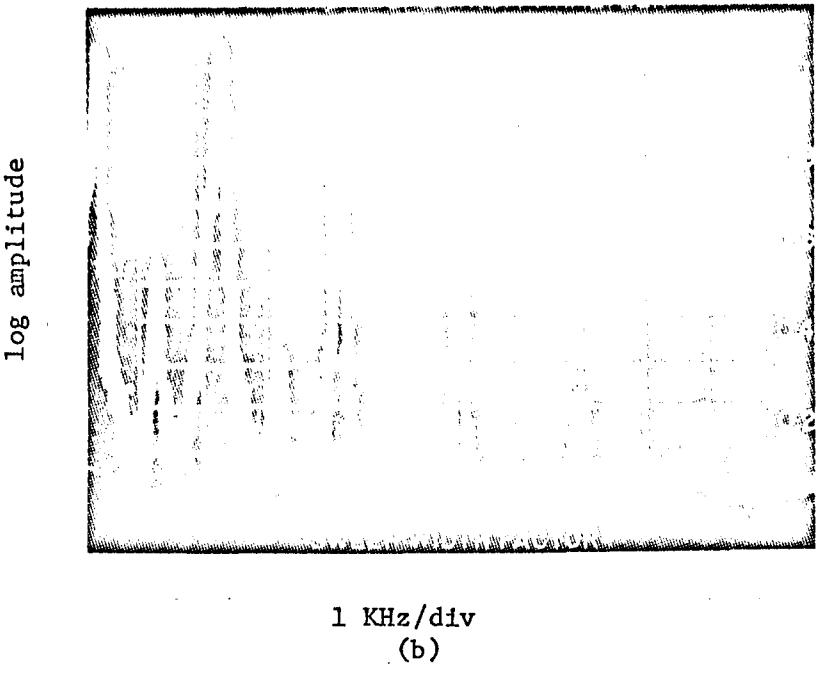

Fig. 4.2.7. Output waveform (a) and spectrum (b) of New Mode without feedback at 1 KHz.

cutoff frequency of 35 KHz. This integrated waveform is presented in Fig. 4.2.8 (a). The spectrum of this waveform, before the R-C filter, is shown in Fig. 4.2.8 (b). Note the similarity between this spectrum and that of Fig. 4.2.7 (b). Due to the higher currents and dissipation which resulted from removing the output filter, the second-harmonic distortion had increased.

As an example of the performance the New Mode without feedback is capable of, when operated directly into a resistive load, Fig. 4.2.9 is presented. This photograph was taken when two much-faster transistors were being used for Q_{18} and Q_{19}. These fast transistors, however, were easily destroyed by almost any transient that happened to occur. After burning out three sets of these transistors, the author decided to use the more rugged 2N1724's. (Also, his supply of fast transistors was depleted!)

The only visible distortion in Fig. 4.2.9 occurs in the region of pulse overlap, near the center. By choosing a much smaller k_d (remember, k_d had been chosen for best performance into an inductive filter) most of this distortion could be eliminated. There is no distortion due to amplitude variation here because, when operating into a resistive load, a constant current always flows through Q_{18} or Q_{19} whenever either one is conducting. This current is approximately 2.4 amperes for an 8 ohm load and a 40 volt supply. (Diodes D_{17} and D_{18} do not conduct in this mode of operation.)

4.2.2 High Frequency Distortion

Table 4.2.2 gives distortion figures for the amplifier with a 4.0

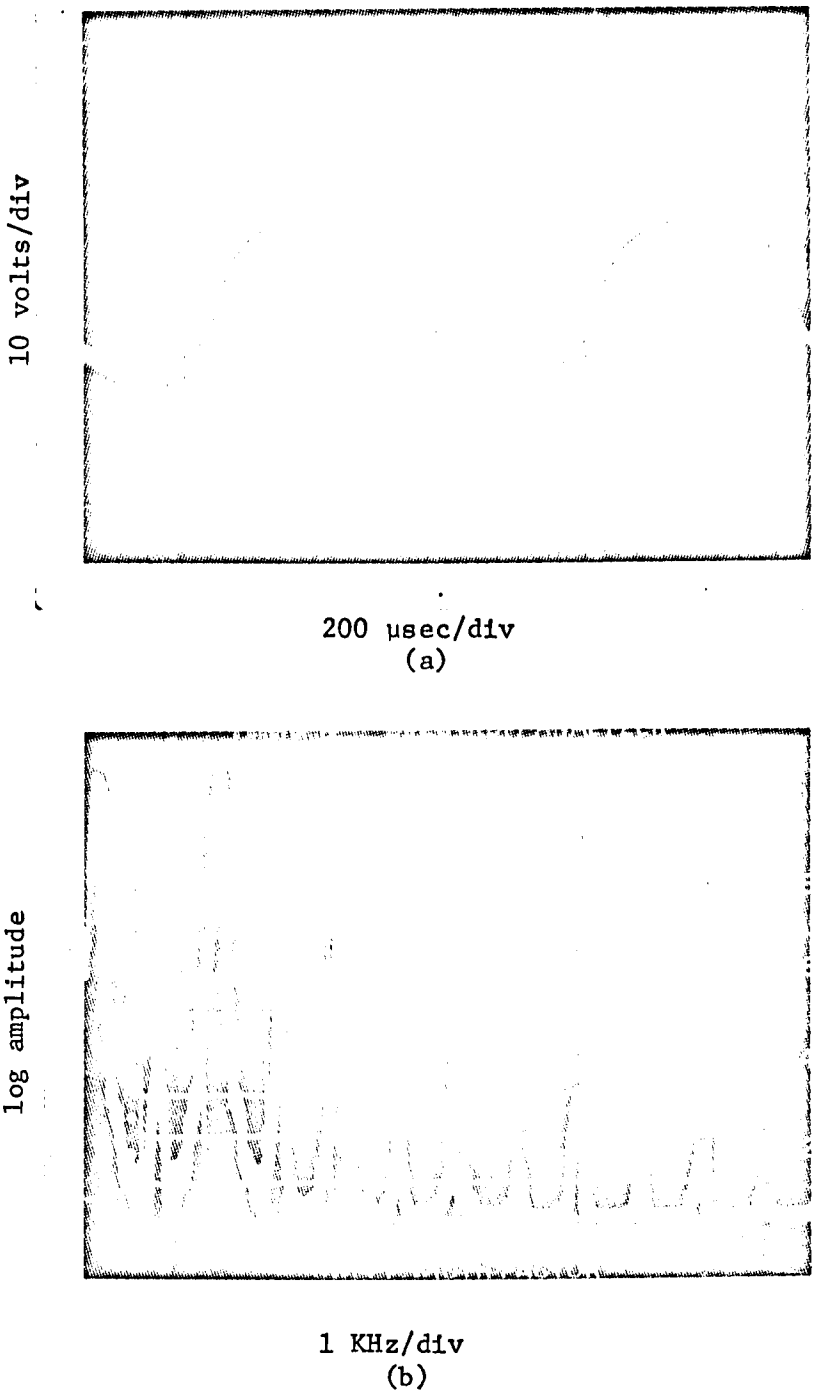

Fig. 4.2.8. Output waveform (a) and spectrum (b) of New Mode without output filter or feedback at 1 KHz. Waveform (a) integrated with low-pass filter before oscilloscope.

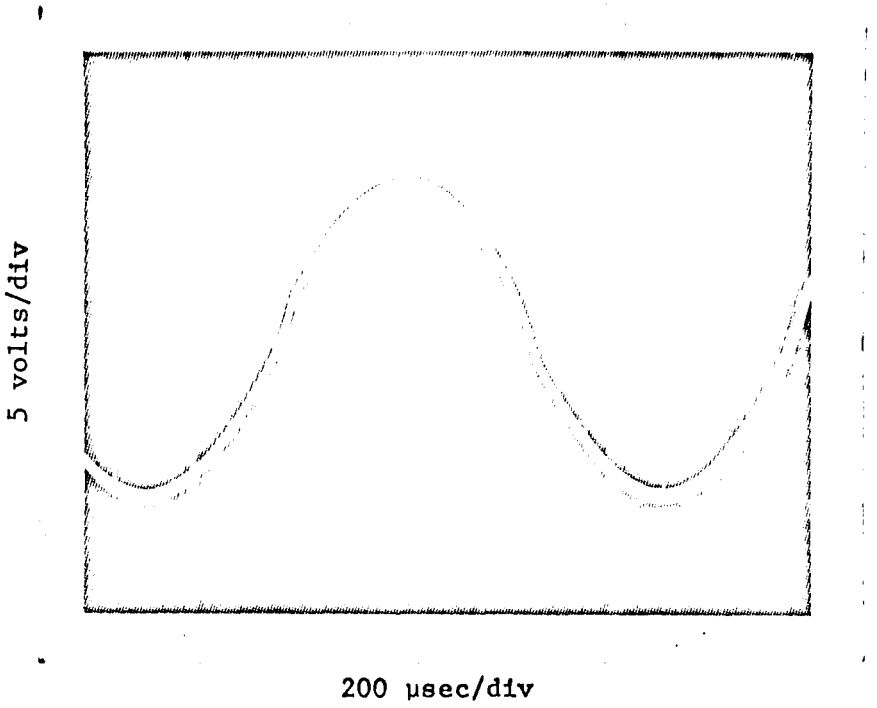

Fig. 4.2.9. Output waveform of New Mode without output filter or feedback, at 500 Hz, with faster output transistors (f_t = 50 MHz). Output voltage = 7 volts RMS.

TABLE 4.2.2

DISTORTION PERFORMANCE OF DUAL-MODE

AMPLIFIER AT 4.0 KHz

Mode	Feedback Position	% Distortion	db Feedback @ 1 KHz
Conv.	3	8.2	0
Conv.	2	5.8	9.9
Conv.	1	1.1	23.3
New	3	15	0
New	2	14	8.9
New	1	3.5	22.0

KHz input signal. The presence of the output filter and the Butterworth filter (Fig. 4.2.2) allows only the fundamental through the fifth harmonic to contribute to the distortion reading. The response of the feedback filter, including C_{21}, makes the feedback less effective at higher frequencies, as a comparison of Tables 4.2.1 and 4.2.2 will indicate. Note that the distortion level of each mode without feedback is approximately independent of frequency.

CHAPTER V

CONCLUSIONS AND RECOMMENDATIONS

This investigation shows that, in spite of the problem of filtering the output, a New Mode amplifier with good performance can be built. An analysis of efficiency and distortion data on the dual-mode amplifier described in this thesis shows that, when operated in the New Mode, this amplifier has somewhat higher efficiency for a given distortion level than it does when operated in the conventional mode. Compare, for example, the New Mode with 22 db feedback and the conventional mode with 9.9 db feedback. At 1 KHz, the New Mode has 1.46% distortion with an efficiency of 52.3%, while the conventional mode has 2.5% distortion with an efficiency of 51.6%.

For purposes of comparison, a home-made Class B amplifier of similar design and operating under similar conditions exhibited an efficiency of 39.5%. This amplifier had a quasi-complementary-symmetry transformer-less output circuit with just enough bias to overcome crossover distortion. The supply voltages, power output and load resistance were, as they were for all measurements on the dual-mode amplifier, 42 volts, 8 watts and 8 ohms, respectively. This measurement was made at 1 KHz.

The New Mode particularly excelled at higher frequencies. At signal frequencies within an octave or two of the output filter cutoff frequency, the higher-harmonic distortion which is characteristic of the New Mode is less of a problem, since these harmonics are subject to the attenuation of the filter. The efficiency of the New Mode remained high at high signal frequencies, thereby making this mode desirable in such applications. Also, the New Mode did not exhibit any thermal runaway

problems, as did the conventional mode, when operating at high signal frequencies.

The New Mode of Class D amplification has two significant disadvantages over the conventional mode: First, its higher level of distortion makes it undesirable in applications requiring a very faithful reproduction of the input signal. Second, the complexity of the system is considerably greater than that of a conventional mode amplifier.

A conventional Class D amplifier can be made very simple, since only one train of width-modulated pulses is involved. Extremely simple self-oscillating designs, which inherently have a very high degree of overall feedback and, therefore, low distortion, can be built using the conventional mode. A good example is K. C. Johnson's [11] low-power circuit, which has only five transistors--no more than necessary for a comparable Class B design!

These simple designs have one significant drawback, however. Their switching frequency is a function of the modulating signal. Under no-signal conditions, the switching frequency is at a maximum, creating additional dissipation in the output transistors. On the peaks of the modulating wave, the switching frequency is reduced greatly, creating additional distortion. These effects have been discussed by Johnson [15].

Fixed-frequency designs such as the eight transistor circuit of Turnbull and Townsend [16] require a considerably greater number of parts, particularly if negative feedback is used. The fixed-frequency New Mode design of Crowhurst [17] requires fourteen transistors, while the design presented in this thesis (remember: this circuit was <u>not</u>

designed for simplicity) uses twenty transistors.

The use of integrated circuits could greatly reduce the size and cost of a New Mode amplifier.

The development of a self-oscillating feedback-type New Mode amplifier (i.e., one which uses the negative feedback loop to generate the switching signal) would eliminate many of the problems associated with the use of feedback in a non-self-oscillating amplifier. This would also eliminate the need for a complicated feedback filter.

LIST OF REFERENCES

[1] Bedford, B. D., "Improvements in and Relating to Electric Amplifying Circuits", U. K. Patent No. 389,855, September 25, 1931.

[2] Birt, D. R., "Modulated Pulse A. F. Amplifiers, An Alternative Approach to the Design of Amplifiers Using Semiconductors, Wireless World. Vol. 69, February, 1963, pp. 76-83.

[3] Crowhurst, Norman H., "Development of Pulse-Modulated Audio Amplification", Audio.Vol. 49, September, 1965, Part I, pp. 19-50; October, 1965, Part II, pp. 32-40; November, 1965, Part III, pp. 36-73; December, 1965, Part IV, pp. 36-59.

[4] Black, Harold S., Modulation Theory. P. Van Nostrand Company, New York, 1953, p. 275.

[5] Lucas, Billy F., "An Investigation of Pulse Duration Modulation", M. S. Thesis, Department of Electrical Engineering, University of Kansas, 1965, p. 10. (Processed under CFSTI No. AD617085)

[6] Ibid., p. 13.

[7] Black, Op. Cit., p. 277.

[8] Ibid., pp. 266-67.

[9] Ibid., pp. 266-70.

[10] MacRobert, Thomas Murray, Spherical Harmonics. 2d ed. rev.; Dover Publications Inc., New York, 1948, p. 251.

[11] Johnson, K. C., "Pulse Modulated A.F. Amplifiers", Wireless World. Vol. 69, March, 1963, p. 135. (Published under Letters to the Editor)

[12] Turnbull, G. F. and J. M. Townsend, "A Feedback Pulse Width Modulated Audio Amplifier", Wireless World. Vol. 71, April, 1965, p. 165.

[13] Josephson, B. D., "Pulse Width Modulated Audio Amplifiers", Wireless World. Vol. 71, July, 1965, pp. 335-36. (Published under Letters to the Editor)

[14] Bach, R. E., Jr. and A. W. Carlson, C. A. Furcinitti, R. E. Scott, "Reliable Solid-State Circuits", Semiannual Report No. 1, NASA NGR-22-011-007, Northeastern University, Boston, July 1, 1965, pp. 30-31.

[15] Johnson, K. C., "Distortions Inherent in P.W.M.", Wireless World. Vol. 74, February, 1968, pp. 672-76.

[16] Turnbull, Op. Cit., p. 162.

[17] Crowhurst, Norman H., "40 Watts in 40 Ounces! The Two-State Amplifier", Radio-Electronics. Vol. 36, August, 1965, p. 36.

APPENDIX A

CIRCUIT DESIGN EQUATIONS

This appendix presents some approximate equations used in the design of the amplifier of Fig. 3.2.1. These equations can be easily derived and, therefore, no derivation is given here.

The following assumptions were made in the derivation of the equations in the appendix:

(1) The saturation resistance of all transistors is negligible,

(2) the base current of all transistors is negligible,

(3) all diodes and transistor base-emitter junctions have the same forward voltage drop at a given temperature, and

(4) all transistors and diodes switch in zero time.

The following definitions apply:

$V_x \equiv$ the dc voltage at point x or across component x.

$v_x \equiv$ the peak-to-peak ac voltage at point x or across component x.

$D \equiv$ the forward voltage drop across a silicon diode ≈ 0.65 volts at room temperature.

$V_{reg} \equiv$ the output dc voltage of the voltage regulator circuit.

$V_{sup} \equiv$ the supply voltage (B+) to the amplifier, which is normally 40 volts.

$R_x \| R_y \equiv$ the parallel combination of resistors R_x and R_y; that is, $R_x R_y / (R_x + R_y)$

The capital letters A, B, and C, when not used as subscripts, refer to Fig. 2.2.1.

Oscillator:

$$\omega_c \approx \frac{1}{R_1 C_1} \approx \frac{1}{R_2 C_2} \approx \frac{1}{(R_3+R_4)C_3} \qquad (A.1)$$

$$V_A \approx \frac{2D\,(R_1+R_2+R_5 \| R_6)}{R_5 \| R_6} \qquad (A.2)$$

First Slicer:

$$\text{Control Value} \approx 4D \qquad (A.3)$$

$$v_B \approx V_{reg} - V_{D_4} \qquad (A.4)$$

Miller Integrator:

$$v_C \approx \frac{2\pi v_B}{4\omega_c R_{15}+R_{13}/2)C_5} \qquad (A.5)$$

Summing Amplifier:

$$B \approx v_C \frac{R_{42} \| R_{43}}{R_{40}} \qquad (A.6)$$

$$A \approx v_E \frac{R_{42} \| R_{43}}{R_{41}} \qquad (A.7)$$

$$C \approx V_{sup} \frac{R_{59}}{R_{53}+R_{54}} \quad \text{(Conventional Mode)} \qquad (A.8)$$

$$C \approx V_{D_{15}} \quad \text{(New Mode)} \qquad (A.9)$$

Voltage Regulator:

$$V_{reg} \approx V_{D_5} + V_{D_6} \tag{A.10}$$

APPENDIX B

COMPUTER PROGRAM AND CALCULATED VALUES

The computer program used in section 3.3 to calculate values of output voltage V_J versus pulse duty cycle K is presented in this appendix. This Fortran IV program uses Eq. (3.3.21) to calculate values of V_{out} for $0.00 \leq K \leq 0.60$, and Eq. (3.3.23) for $0.61 \leq K \leq 1.00$. These values are shown in Table B.1.

This program is:

```
      DIMENSIØN C(101), V(101)
      WRITE (6,5)
      C(1) = 0
      DØ 3 I = 1,101
      C(I+1) = C(I)+.01
      IF (62-I) 2,2,1
1     V(I)= -10,-12.9*C(I)**2+10.*SQRT(1.+6.45*C(I)**2+1.664*C(I)**4
      GØ TØ 3
2     V(I)= 40.+C(I)-20.
3     WRITE (6,4)I,C(I),V(I)
4     FØRMAT (I5,F9.2,F12.4)
5     FØRMAT (12X,1HK,6X,5HV OUT,//)
      END
```

TABLE B.1

COMPUTER-CALCULATED VALUES OF K AND V_{OUT}

K	V_{OUT}	K	V_{OUT}	K	V_{OUT}
0.00	-0.0000	0.34	1.8048	0.68	7.2000
0.01	0.0019	0.35	1.8923	0.69	7.6000
0.02	0.0077	0.36	1.9805	0.70	8.0000
0.03	0.0174	0.37	2.0694	0.71	8.4000
0.04	0.0308	0.38	2.1589	0.72	8.8000
0.05	0.0481	0.39	2.2490	0.73	9.2000
0.06	0.0691	0.40	2.3395	0.74	9.6000
0.07	0.0938	0.41	2.4304	0.75	10.0000
0.08	0.1221	0.42	2.5216	0.76	10.4000
0.09	0.1539	0.43	2.6131	0.77	10.8000
0.10	0.1893	0.44	2.7048	0.78	11.2000
0.11	0.2280	0.45	2.7967	0.79	11.6000
0.12	0.2700	0.46	2.8887	0.80	12.0000
0.13	0.3152	0.47	2.9807	0.81	12.4000
0.14	0.3635	0.48	3.0728	0.82	12.8000
0.15	0.4147	0.49	3.1648	0.83	13.2000
0.16	0.4689	0.50	3.2568	0.84	13.6000
0.17	0.5258	0.51	3.3487	0.85	14.0000
0.18	0.5853	0.52	3.4404	0.86	14.4000
0.19	0.6474	0.53	3.5319	0.87	14.8000
0.20	0.7119	0.54	3.6232	0.88	15.2000
0.21	0.7787	0.55	3.7142	0.89	15.6000
0.22	0.8477	0.56	3.8050	0.90	16.0000
0.23	0.9187	0.57	3.8954	0.91	16.4000
0.24	0.9917	0.58	3.9855	0.92	16.8000
0.25	1.0665	0.59	4.0753	0.93	17.2000
0.26	1.1431	0.60	4.1647	0.94	17.6000
0.27	1.2212	0.61	4.4000	0.95	18.0000
0.28	1.3009	0.62	4.8000	0.96	18.4000
0.29	1.3819	0.63	5.2000	0.97	18.8000
0.30	1.4643	0.64	5.6000	0.98	19.2000
0.31	1.5479	0.65	6.0000	0.99	19.6000
0.32	1.6325	0.66	6.4000	1.00	20.0000
0.33	1.7182	0.67	6.8000		

The vita has been removed from the scanned document

A NEW MODE OF CLASS D AMPLIFICATION

by

Philip M. Cowett, Jr.

ABSTRACT

With the current trend in electronics toward microminiaturization, there is a need for a more efficient method of power amplification. Class D operation, in which the output transistors are either cut off or saturated and, hence, dissipate very little power, is one method of satisfying this need. This paper presents a study of a new mode of Class D amplification.

In a conventional Class D amplifier, one transistor is always on and one transistor is always off. In a New Mode Class D amplifier both transistors are off most of the time, reducing unwanted dissipation in the output transistors, filter and load. The output of a New Mode amplifier consists of positive and negative trains of width-modulated pulses. For a positive-going output, the positive pulses increase in width while the negative ones disappear.

While the New Mode is theoretically capable of distortion performance as good as or better than the conventional mode, problems in filtering the output prevent it from obtaining this performance. These problems are caused by the infinite impedance presented to the filter during the time when both transistors are off. However, the addition of negative feedback and a "damping" resistor to the filter reduce distortion to a level tolerable in most applications.

The New Mode of Class D amplification proved to be slightly more efficient than the conventional mode, and considerably more efficient than Class B amplification.